

Electronic Supplementary Information

Metal-free photocatalysis at charged aqueous interface: boosting the photocatalytic oxidative coupling of arylamines to azoaromatics under ambient conditions

Shivendra Singh,[‡] Vidhi Agarwal,[‡] Tridib K. Sarma,^{*} and Tushar Kanti Mukherjee^{*}

Table of Contents

1.	Materials	S3
2.	Methods and Supporting Figures	S3–S24
3.	^1H and ^{13}C NMR data	S25–S37
4.	GC-MS Spectra	S38–S50
5.	Supporting Tables	S51–S54
6.	References	S55

Experimental Section

Materials

Cetyltrimethylammonium bromide (CTAB), sodium dodecyl sulfate (SDS), TritonX-100 (TX-100), and potassium phosphate (K_3PO_4) were purchased from Sigma-Aldrich. H_2O_2 test strips (MQuant test peroxide) were purchased from Supelco, Sigma-Aldrich. *p*-chloroaniline, 5,5-dimethyl-1-pyrroline N-oxide (DMPO), and *p*-toluidine were procured from TCI. Eosin yellow (Eosin Y/EY), 1,4-diazabicyclo[2.2.2]octane (DABCO), potassium hydroxide (KOH), *p*-anisidine, *p*-bromoaniline, 3,4-dimethylaniline, aniline, and phosphotungstic acid (PTA) were procured from SRL, India. 3,5-dimethoxyaniline, 5,6,7,8-tetrahydro-2-naphthylamine, and *o*-methoxyaniline hydrochloride were procured from BLD Pharmatech, India. *p*-nitroaniline, *p*-phenylenediamine (PPD), and *o*-phenylenediamine (OPD) were procured from Loba Chemie, India. Milli-Q water was obtained from a Millipore water purifier system (Milli-Q integral).

Absorption and Emission Measurements

Absorption spectra were obtained using a Perkin Elmer UV/vis/NIR spectrophotometer (Perkin-Elmer Lambda 750) and emission spectra were obtained using Fluoromax-4 spectrofluorometer (HORIBA Jobin Yvon). The spectral measurements were carried out in a $1 \times 1 \text{ cm}^2$ quartz cuvette.

Interactions of EY with Different Surfactants

The interactions of negatively charged EY were studied with different surfactants like CTAB (positively charged), SDS (negatively charged), and TX-100 (neutral). Initially, $2 \mu\text{M}$ EY was added to the different concentrations of CTAB (0–10 mM) and the solution was incubated for 10 min before taking any measurements. Subsequently, the absorption spectra of the above mixtures were recorded. Similarly, the emission spectra of the EY@CTAB mixtures were recorded by exciting the samples at $\lambda_{\text{ex}} = 510 \text{ nm}$, and the emission was recorded in the range of 520–700 nm.

Time-Correlated Single Photon Counting Measurements

The fluorescence lifetime decays were obtained on a HORIBA Jobin Yvon picosecond time-correlated single photon counting (TCSPC) spectrometer (Fluorocube-01-NL model). A dilute Ludox solution was utilized to record the instrument response function (IRF). All the decay traces were collected using a photomultiplier tube (TBX-07C) and were then analyzed with IBH DAS 6.0 software according to the literature reports.¹ The EY and EY@CTAB samples were excited using a 482 nm picosecond diode laser and emission was collected at 535 and 545 nm, respectively.

Transmission Electron Microscopy Measurements

Transmission electron microscopy (TEM) measurements were performed using a 200 kV UHR FEG-TEM microscope (JEOL, Model JEM 2100F). The CTAB micellar solution was prepared in pH 7.4 aqueous solution. The sample was dropcasted over a carbon-coated copper TEM grid and was negatively stained using one drop of 1% (w/v) PTA. Finally, the excess staining agent was removed by washing with Milli-Q water and the sample was dried at room temperature under an IR lamp.

Procedure for Synthesis of Azo Compounds

Initially, 40 mM CTAB micellar solution was prepared by dissolving an appropriate amount of CTAB in 5 mL Milli-Q water. Subsequently, 0.6 mol% Eosin Y was added to the above solution and equilibrated for 5 minutes. Next, 0.05 mmol amine substrate and 2 equiv. K_3PO_4 were added to the above solution. The reaction mixture was then irradiated for 4 h with green LED ($\lambda = 525$ nm) inside a homemade photocatalytic reactor equipped with a portable fan under ambient conditions. The reaction mixture was extracted with diethyl ether after completion and washed several times with water and then dried using anhydrous sodium sulfate. The solvent was evaporated using a rotary evaporator and then the residue obtained was purified using a silica gel column and the obtained product was air-dried overnight for NMR analysis.

Fluorescence Quenching Experiments

Fluorescence quenching experiments were carried out with the EY@CTAB micellar system. Typically, 2 μ M EY solution was added to a 1 mM CTAB solution at room temperature. Subsequently, different substrates were added to the above micellar solution by varying their concentrations. The above mixture was then equilibrated for 5 min before recording the fluorescence spectra. The solutions were excited at 510 nm. For the quenching experiments in the presence of a base, 0.2 mM K_3PO_4 was added to the solution before the addition of substrates. Quenching rate constants were calculated from the S_V constant by considering a fluorescence lifetime of 2.74 ns for EY@CTAB using the following equation:

$$K_{SV} = k_q \times \tau \quad (1)$$

Fluorescence Up-Conversion Experiments

Ultrafast fluorescence decays were obtained using fluorescence up-conversion, widely known as femtosecond optical gating (FOG) with a FOG100 spectrometer from CDP corporation, Russia as discussed in earlier literature reports.² Briefly 800 nm, 100 fs pulses from a mode-locked Ti:sapphire oscillator (Tsunami, Spectra Physics), with 80 MHz repetition rate, pumped by a 4.2 W Millennia (Spectra Physics) DPSS laser, were focused on a non-linear crystal (NC1, 0.5 mm b-BBO, $\gamma = 251$, $f = 901$) to generate second harmonic 400 nm excitation light, which was used to excite the solutions of EY@CTAB and EY@CTAB in the presence of *p*-anisidine in a rotating cell with a 1 mm pathlength. Residual 800 nm light (gate) was focused, along with fluorescence from the sample on another nonlinear crystal (NC2, 0.5 mm BBO, $\gamma = 381$, $f = 901$), to generate an up-converted signal. This was dispersed by a double grating monochromator and detected by a photomultiplier tube at different path differences between the gate and fluorescence signal, to generate transient fluorescence. The decays were recorded at magic angle polarization with respect to the excitation pulse and were fitted with iterative reconvolution, using an Igor Pro routine.²

Gas Chromatography-Mass Spectrometry Measurements

Gas chromatography-mass spectrometry (GC-MS) spectra were recorded using a Shimadzu GC-MS, QP2010 mass spectrometer with a 30 m long Rxi-5Sil MS separation column with a 0.25 mm diameter and 0.25 μ M thickness. The column oven temperature was set at 40 $^{\circ}C$ for 5 min, followed by a 20 $^{\circ}C$ /min ramp to 280 $^{\circ}C$ and held for 8 min.

Nuclear Magnetic Resonance Measurements

AVANCE NEO Ascend 500 Bruker BioSpin, a 500 MHz spectrometer was used to record ^1H and ^{13}C nuclear magnetic resonance (NMR) spectra. Data for ^1H NMR spectra are reported as chemical shift (δ ppm), multiplicity (s = singlet, d = doublet, t = triplet, m = multiplet), coupling constant (J Hz) and integration whereas assignment data for ^{13}C NMR spectra are reported as chemical shift.

H₂O₂ Detection

The H₂O₂ detection experiment was carried out under the standard optimized reaction conditions. Briefly, in 5 ml CTAB solution (40 mM), 0.6 mol% EY was added and incubated for 5 min. Subsequently, 0.05 mmol *p*-anisidine and 2 equiv. K₃PO₄ were added to the above solution and irradiated under green light for 4 h. Finally, 10-20 μl of the reaction mixture was dropped over the H₂O₂ test strips (MQuant test peroxide) to check the presence of H₂O₂.

Cyclic Voltammetry (CV) Experiments

The Glassy Carbon electrode (GCE) was cleaned using alumina slurry on a clean micro cloth pad to get a clear glossy surface. The cleaned GCE was further sonicated in methanol and water. For the CV measurements, all the solutions of EY (12 μM), CTAB (12 mM), EY@CTAB mixture, and different substrates (10 mM) were prepared in pH 7.4 phosphate buffer. The CV measurements were carried out on a CHI1103C electrochemical analyzer by using clean bare GCE as working electrodes, platinum wire as a counter electrode, and pseudo Ag|AgCl as a reference electrode. The CV measurements were carried out at a scan rate of 100 mV/s. To convert the redox potentials from vs Ag/AgCl to vs SCE, a factor of -0.045 V was added to the redox potentials obtained from CV measurements. During the whole study, 10 mM pH 7.4 phosphate buffer was utilized as an electrolyte.

Calculation of Excited-State Reduction Potential

The excited-state reduction potential of EY@CTAB ($E_{1/2}(\text{PC}^*/\text{PC}^{\bullet-})$) was estimated using earlier reported literature.³

$$E_{\text{red}}^* = E_{\text{red}} + E_{0,0} \quad (2)$$

Briefly, we first estimated the zero-zero transition energy ($E_{0,0}$) for EY@CTAB using UV-vis and fluorescence spectroscopy (Fig. S1). Notably, the intersection point at 533 nm of the absorption and emission spectrum of EY@CTAB corresponds to $E_{0,0}$. The $E_{0,0}$ was converted to electrode potential using the equation,

$$E = \frac{hc}{\lambda} \quad (3)$$

The $E_{0,0}$ for the EY@CTAB was estimated to be 2.33 V while the ground state reduction potential of EY@CTAB was found to be 1.03 V using CV measurements (Figure S15). Subsequently, utilizing equation 2, the excited state reduction potential of EY@CTAB was estimated to be 1.33 V.

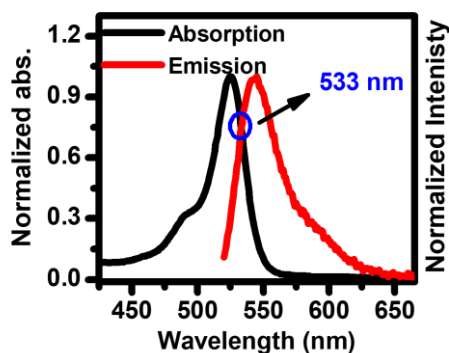


Fig. S1 Estimation of the zero-zero transition energy ($E_{0,0}$) of EY@CTAB from normalized UV-vis and emission spectra.

Scalability Experiments

To show the scalability of our present approach, we performed two sets of scaled up reactions. Initially, the photocatalytic oxidative coupling reaction was performed with 1 mmol *p*-anisidine in 100 ml of water in the presence of 40 mM CTAB, 0.6 mol% EY, and 2 equiv. K_3PO_4 under the irradiation of 1 green LED (44 W). In the second set, the reaction was performed with 5 mmol *p*-anisidine in 500 ml of water under standard reaction conditions using 4 green LEDs (44 W).

Radical Trapping Experiment

Briefly, in 5 ml CTAB solution (40 mM), 0.6 mol% EY was added and incubated for 5 min. Subsequently, 0.05 mmol *p*-anisidine and 2 equiv. K_3PO_4 were added to the above solution and irradiated under green light. After 5 mins of irradiation, 1 equiv. 2,6-Di-tert-butyl-4-methylphenol (BHT) was added to the above reaction mixture to trap the radical. Subsequently, the above mixture was irradiated with a green light for 4 h. The solution obtained was utilized for the HR-MS and GC-MS analysis.

Electron Paramagnetic Resonance (EPR) Experiment

EPR spectra were recorded on a Bruker EMX MicroX spectrometer to confirm the presence of reactive oxygen species (ROS). Briefly, a reaction was set up under standard conditions with 10 mM *p*-anisidine as the substrate. Initially, the reaction was performed for 5 minutes under green light irradiation and subsequently 20 mM 5,5-dimethyl-1-pyrroline N-oxide was added to the reaction mixture to trap the superoxide radical. Subsequently, 500 μ L aliquots were taken from the reaction mixture at 15 and 60 min intervals. The aliquots were then transferred to a quartz EPR tube and analyzed at 150 K.

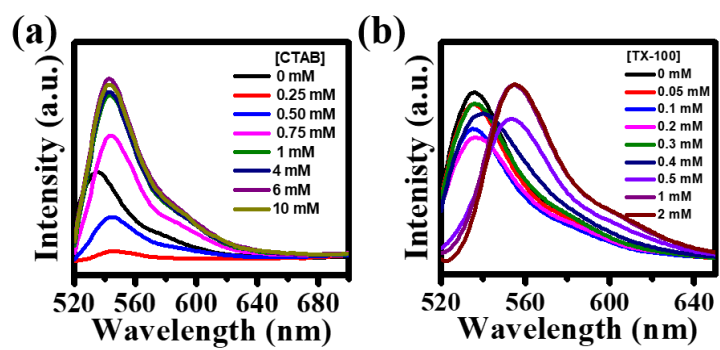


Fig. S2 Changes in the fluorescence spectra of EY in the presence of different concentrations of (a) CTAB, and (b) TX-100.

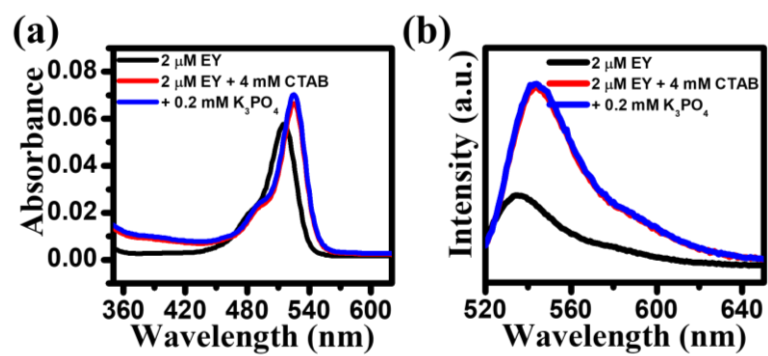


Fig. S3 Changes in the (a) absorption, and (b) fluorescence spectra of EY in the absence and presence of 4 mM CTAB and 0.2 mM K_3PO_4 .

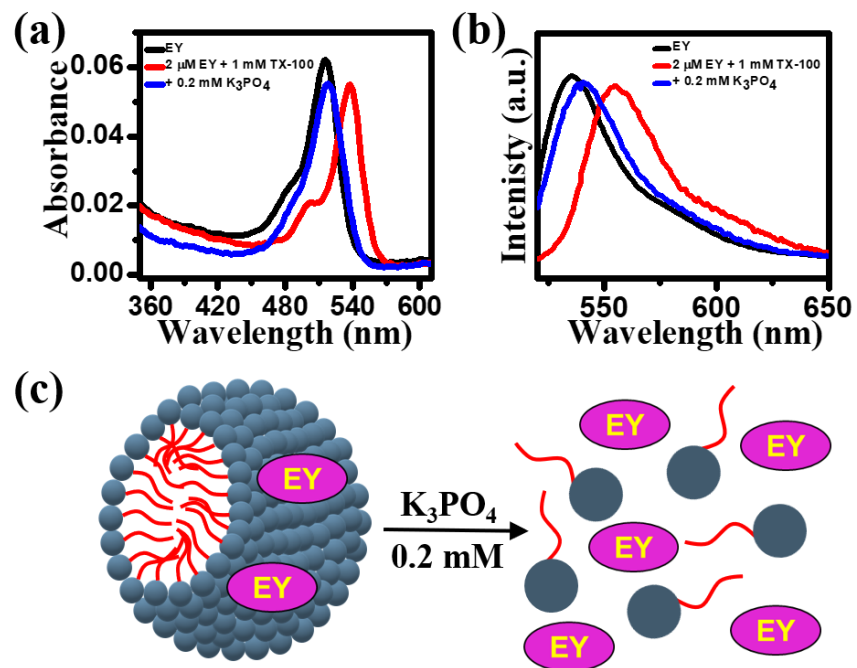


Fig. S4 Changes in the (a) absorption, and (b) fluorescence spectra of 2 μM EY in the absence and presence of 1 mM TX-100 and 0.2 mM K₃PO₄. (c) Schematic representation of the disassembly of TX-100 micelles after the addition of 0.2 mM K₃PO₄.

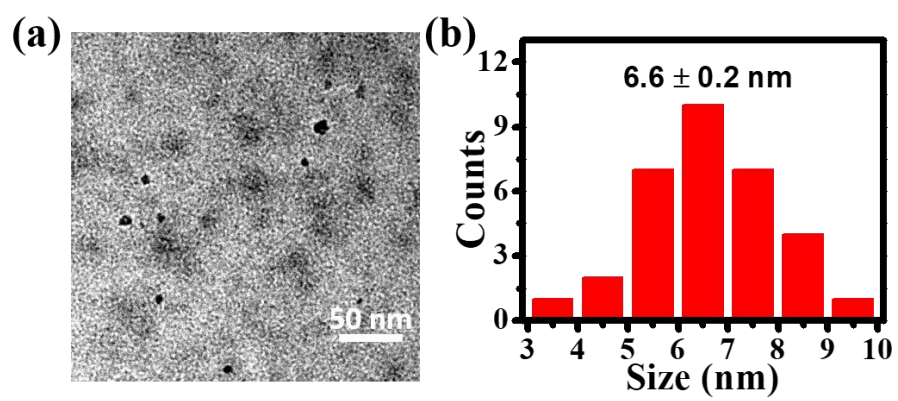


Fig. S5 (a) HRTEM image of CTAB micelles at a CTAB concentration of 40 mM, and (b) the size distribution histogram.

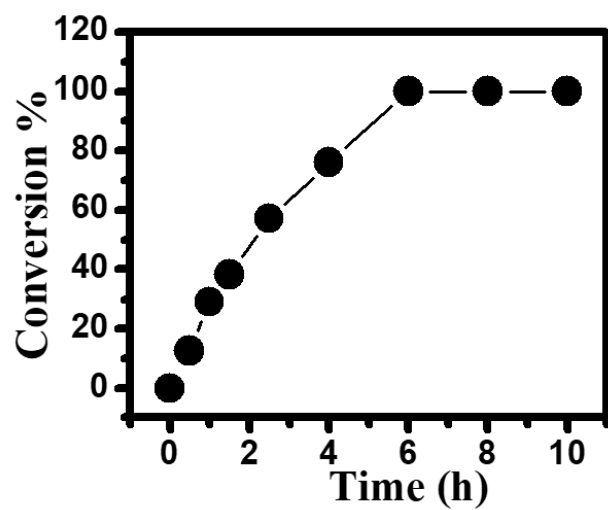


Fig. S6 Plot of conversion yield of *p*-anisidine to 1,2-bis(4-methoxyphenyl)diazene as a function of reaction time under blue light irradiation for 6 h at standard reaction conditions.

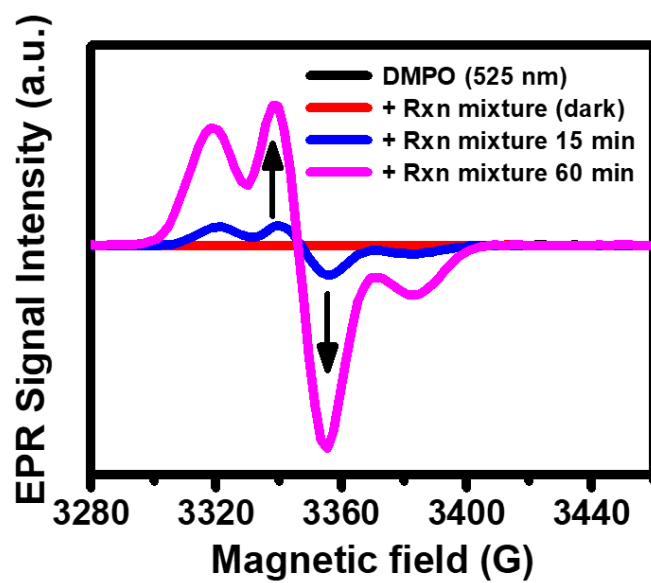


Fig. S7 Changes in the EPR spectra of DMPO (20 mM) in the absence and presence of reaction mixture at 15 min and 60 min time intervals under green LED (44 W) irradiation in the presence of 10 mM *p*-anisidine, 40 mM CTAB, 0.6 mol% EY, and 2 equiv. K_3PO_4 .

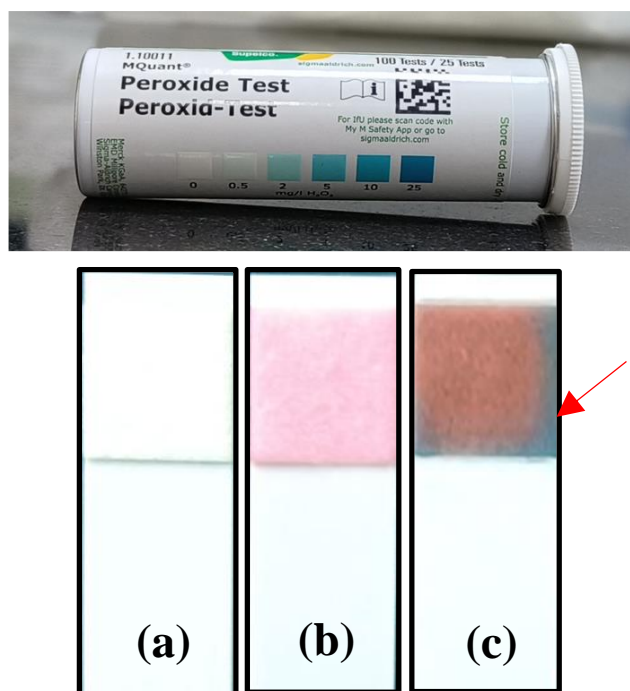


Fig. S8 Daylight photographs of peroxide test strips for (a) blank strips without any measurement, (b) before the photocatalytic experiment, and (c) after 4 h of reaction (EY@CTAB + *p*-anisidine + K_3PO_4) under standard reaction conditions. The red arrow indicates the desired color change of the strip.

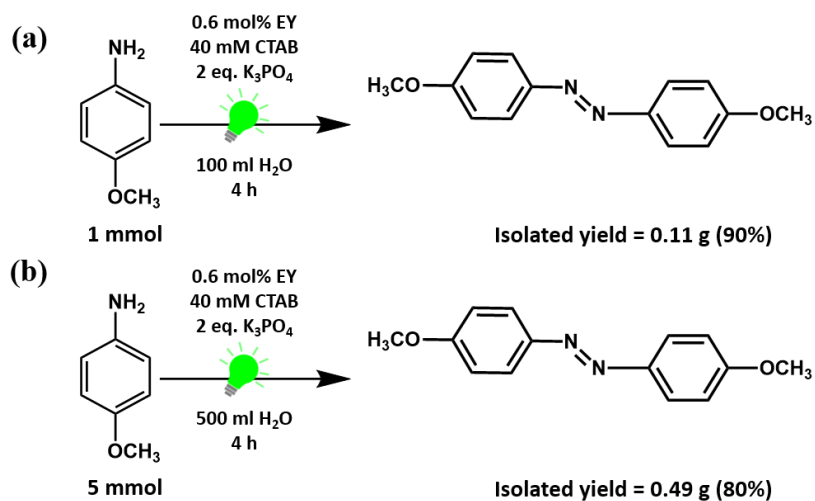


Fig. S9 Schematic representation of scalability experiment for the photocatalytic oxidative coupling of *p*-anisidine to its corresponding azo compound.

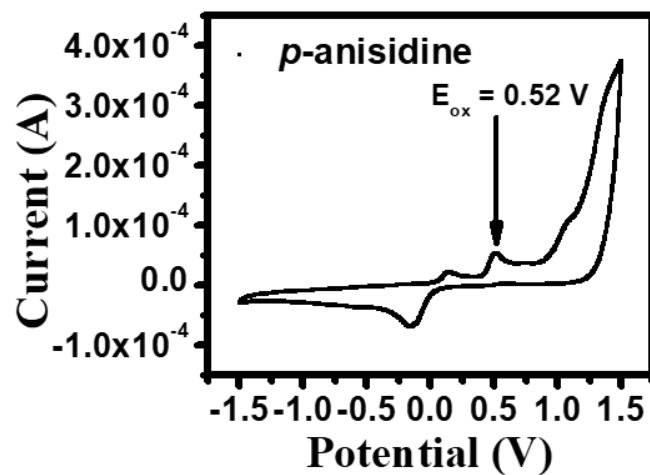


Fig. S10 Cyclic voltammogram of *p*-anisidine (2 mM) in 12 mM CTAB solution carried out at a scan rate of 100 mV/s versus Ag/AgCl electrode.

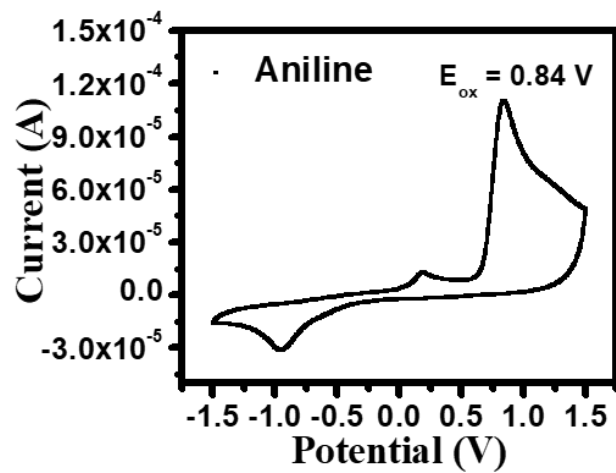


Fig. S11 Cyclic voltammogram of aniline (2 mM) in 12 mM CTAB solution carried out at a scan rate of 100 mV/s versus Ag/AgCl electrode.

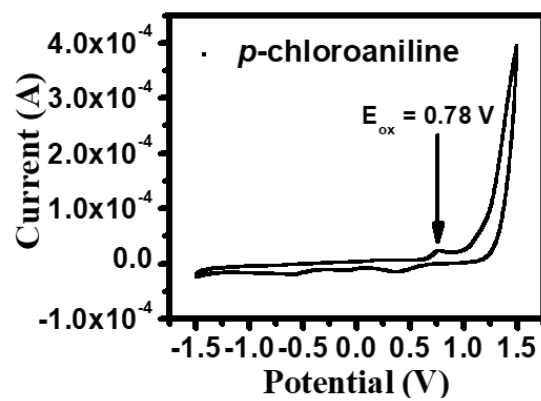


Fig. S12 Cyclic voltammogram of *p*-chloroaniline (2 mM) in 12 mM CTAB solution carried out at a scan rate of 100 mV/s versus Ag/AgCl electrode.

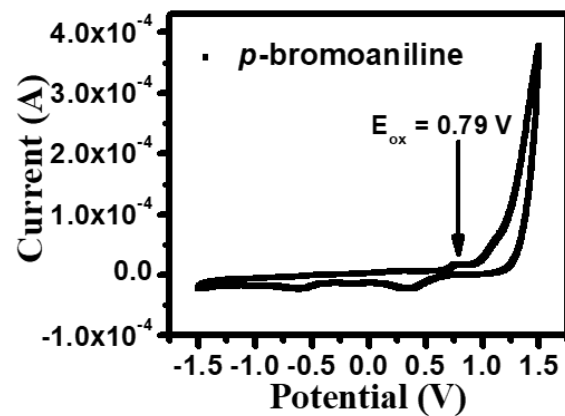


Fig. S13 Cyclic voltammogram of *p*-bromoaniline (2 mM) in 12 mM CTAB solution carried out at a scan rate of 100 mV/s versus Ag/AgCl electrode.

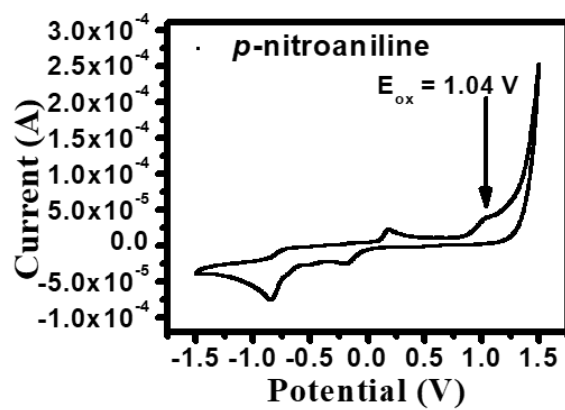


Fig. S14 Cyclic voltammogram of *p*-nitroaniline (2 mM) in 12 mM CTAB solution carried out at a scan rate of 100 mV/s versus Ag/AgCl electrode.

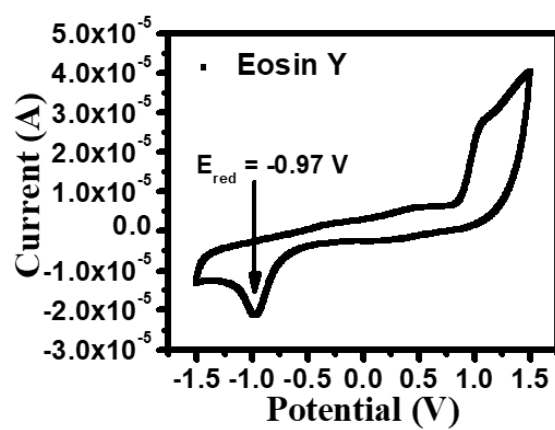


Fig. S15 Cyclic voltammogram of Eosin Y ($12 \mu\text{M}$) in 12 mM CTAB solution carried out at a scan rate of 100 mV/s versus Ag/AgCl electrode.

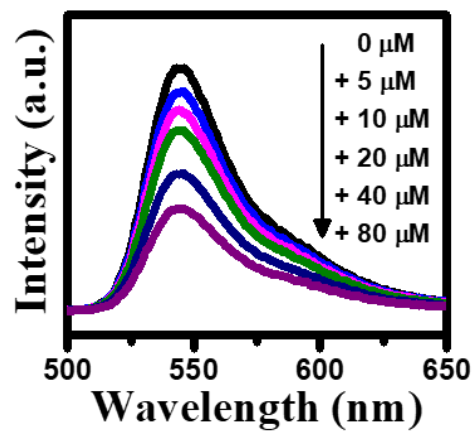


Fig. S16 Fluorescence quenching of EY@CTAB with the gradual addition of different concentrations of *p*-anisidine.

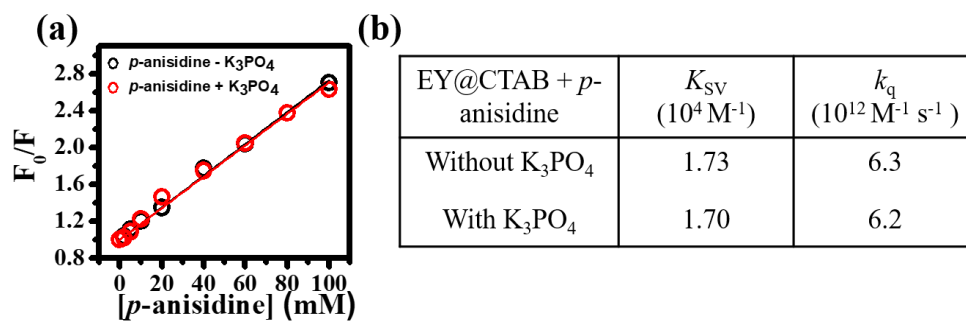


Fig. S17 (a) Steady-state Stern–Volmer plot of EY@CTAB upon addition of different concentrations of *p*-anisidine in the absence and presence of 0.2 mM K_3PO_4 , and (b) chart showing the quenching parameters (K_{SV} and k_q).

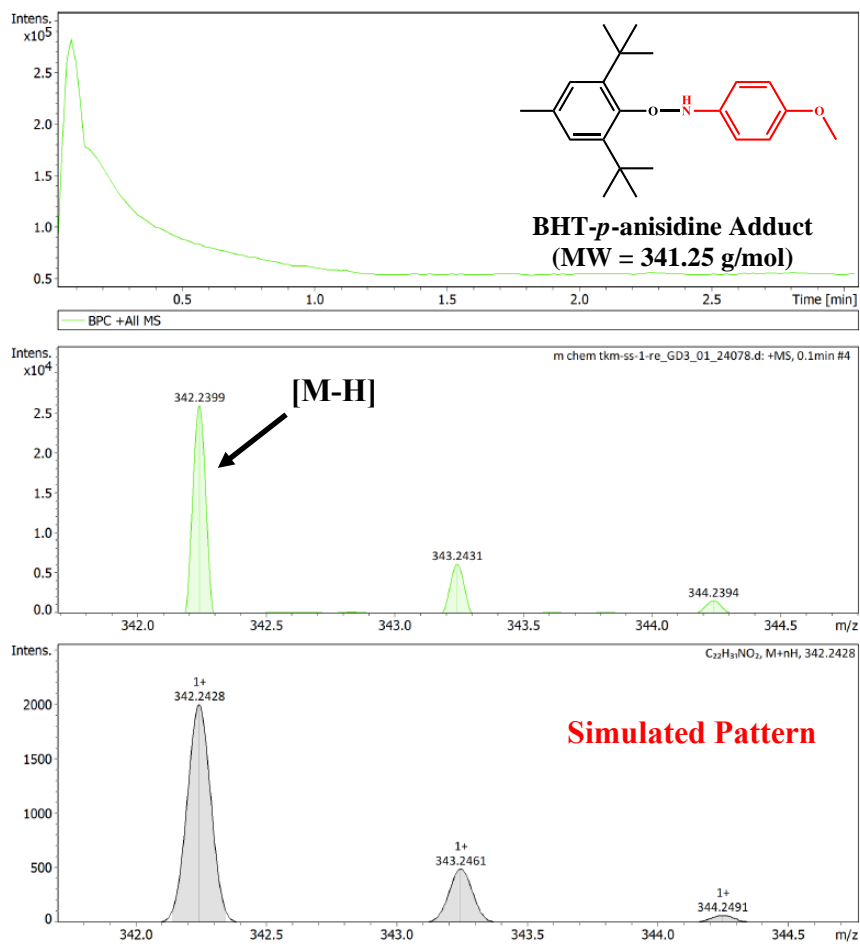


Fig. S18 HR-MS spectra of BHT-*p*-anisidine adduct obtained after radical trap experiment.

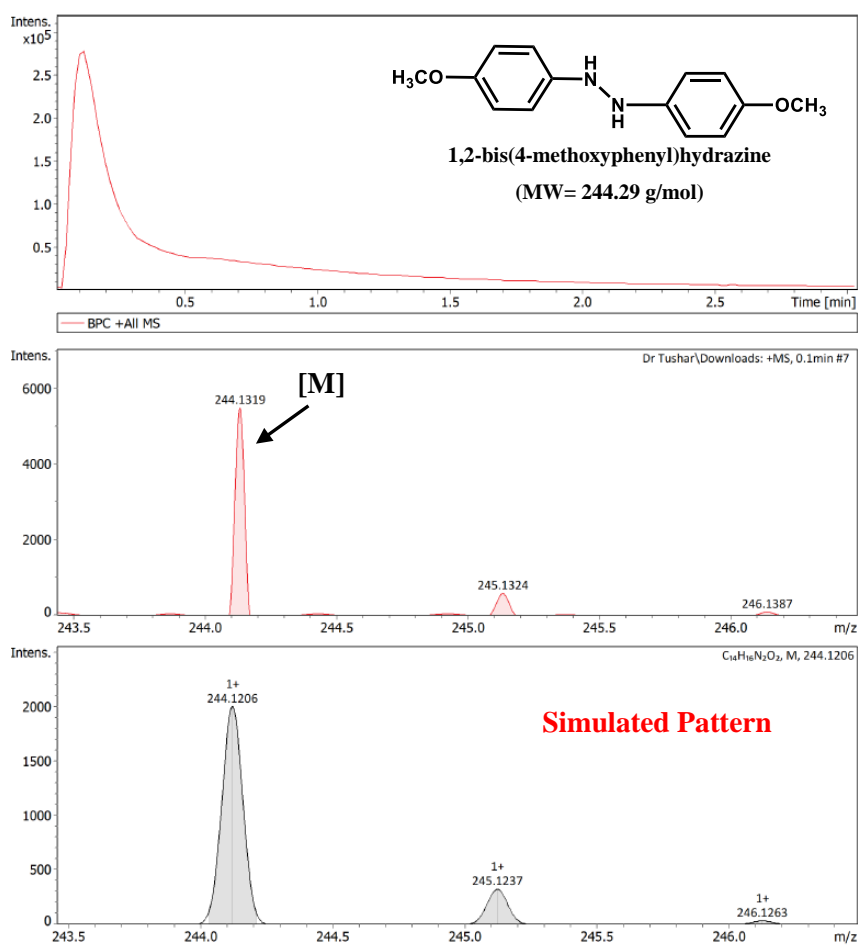
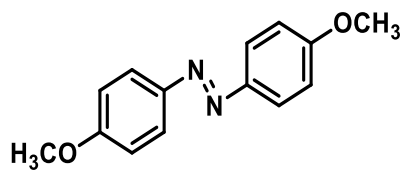
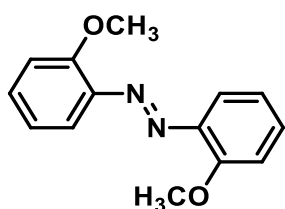


Fig. S19 LC-MS spectra of intermediate 1,2-bis(4-methoxyphenyl)hydrazine (hydrazobenzene) obtained during the photo-oxidative coupling to *p*-anisidine to its corresponding azo compound.

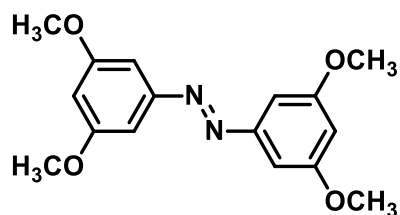
List of ^1H and ^{13}C NMR data



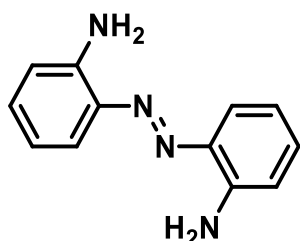
The isolated product was red solid, 11.5 mg, 94% yield. ^1H NMR (500 MHz, Chloroform-*d*) δ 7.95 (d, $J = 8.9$ Hz, 4H), 7.02 (d, 4H), 3.90 (s, 6H). ^{13}C NMR (126 MHz, CDCl_3) δ 161.82, 146.55, 124.59, 114.25, 55.59.



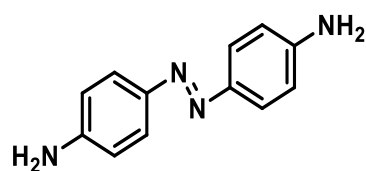
The isolated product was red solid, 11.0 mg, 90% yield. ^1H NMR (400 MHz, Chloroform-*d*) δ 7.63 (d, $J = 7.8$ Hz, 2H), 7.43 (t, $J = 7.6$ Hz, 2H), 7.08 (d, $J = 8.3$ Hz, 2H), 7.00 (t, 2H), 4.02 (s, 6H). ^{13}C NMR (101 MHz, CDCl_3) δ 156.57, 142.69, 131.92, 120.55, 117.28, 112.25, 56.06.



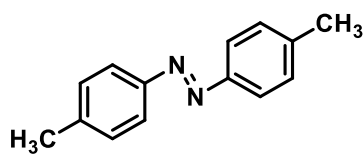
The isolated product was red solid, 14.1 mg, 92% yield. ^1H NMR (500 MHz, Chloroform-*d*) δ 7.15 (s, 4H), 6.60 (s, 2H), 3.88 (s, 12H). ^{13}C NMR (126 MHz, CDCl_3) δ 160.82, 154.01, 103.77, 100.67, 55.34.



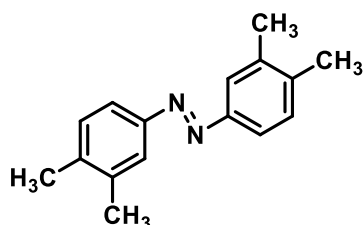
The isolated product was yellow solid, 9.2 mg, 86% yield. ^1H NMR (500 MHz, Chloroform-*d*) δ 7.69 (d, $J = 8.0$ Hz, 2H), 7.19 (t, 2H), 6.80 (t, 2H), 6.77 (d, 2H), 5.49 (s, 4H). ^{13}C NMR (126 MHz, CDCl_3) δ 142.89, 137.50, 131.16, 124.07, 117.43, 116.82.



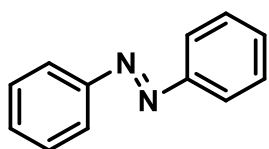
The isolated product was a reddish-orange solid, 9.6 mg, 89% yield. ^1H NMR (500 MHz, Chloroform-*d*) δ 7.74 (d, $J = 8.7$ Hz, 4H), 6.74 (d, $J = 8.7$ Hz, 4H). ^{13}C NMR (126 MHz, CDCl_3) δ 148.75, 146.04, 124.59, 115.02.



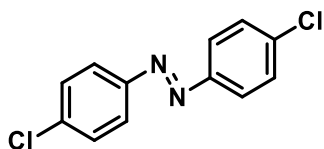
The isolated product was a yellow solid, 10 mg, 94% yield. ^1H NMR (500 MHz, Chloroform-*d*) δ 7.83 (d, J = 8.3 Hz, 4H), 7.32 (d, J = 8.1 Hz, 4H), 2.44 (s, 6H). ^{13}C NMR (126 MHz, CDCl_3) δ 151.09, 141.48, 129.98, 122.99, 21.75.



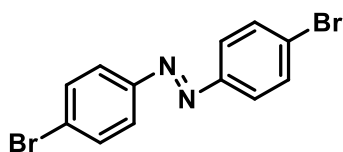
The isolated product was an orange solid, 10.8 mg, 89% yield. ^1H NMR (500 MHz, Chloroform-*d*) δ 7.61 (s, 2H), 7.59 (d, J = 8.0 Hz, 2H), 7.19 (d, J = 7.8 Hz, 2H), 2.28 (s, 6H), 2.26 (s, 6H). ^{13}C NMR (126 MHz, CDCl_3) δ 150.79, 139.45, 136.95, 129.82, 122.90, 120.31, 19.46.



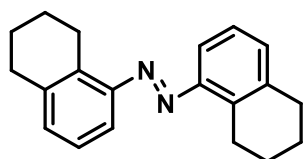
The isolated product was an orange solid, 8.2 mg, 89% yield. ^1H NMR (500 MHz, Chloroform-*d*) δ 7.94 (d, J = 8.5 Hz, 4H), 7.54 – 7.51 (m, 4H), 7.49 – 7.46 (m, 2H). ^{13}C NMR (126 MHz, CDCl_3) δ 152.53, 130.85, 128.95, 122.71.



The isolated product was yellow solid, 11.3 mg, 89% yield. ^1H NMR (500 MHz, Chloroform-*d*) δ 7.87 (d, J = 8.7 Hz, 4H), 7.50 (d, 4H). ^{13}C NMR (126 MHz, CDCl_3) δ 150.78, 137.22, 129.39, 124.18.



The isolated product was an orange solid, 14.6 mg, 85% yield. ^1H NMR (500 MHz, Chloroform-*d*) δ 7.80 (d, J = 8.7 Hz, 4H), 7.66 (d, J = 8.7 Hz, 4H). ^{13}C NMR (126 MHz, CDCl_3) δ 151.13, 132.39, 125.75, 124.40.



The isolated product was a reddish-orange solid, 13.1 mg, 89% yield. ^1H NMR (500 MHz, Chloroform-*d*) δ 7.64 (d, J = 8.3 Hz, 2H), 7.61 (d, J = 5.5 Hz, 2H), 7.19 (d, J = 8.2 Hz, 2H), 2.85 (d, J = 17.4 Hz, 8H), 1.86 – 1.82 (m, 8H). ^{13}C NMR (126 MHz, CDCl_3) δ 150.70, 140.33, 137.76, 129.60, 123.16, 119.73, 29.41, 22.93.

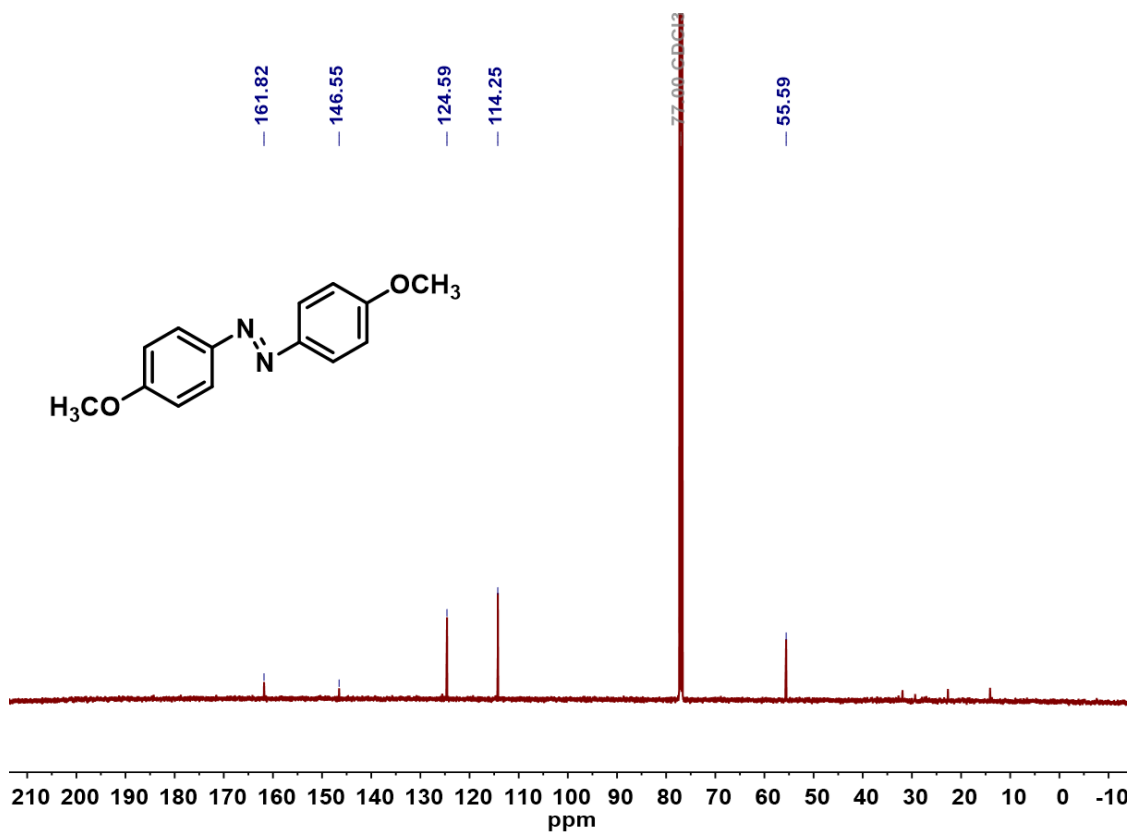
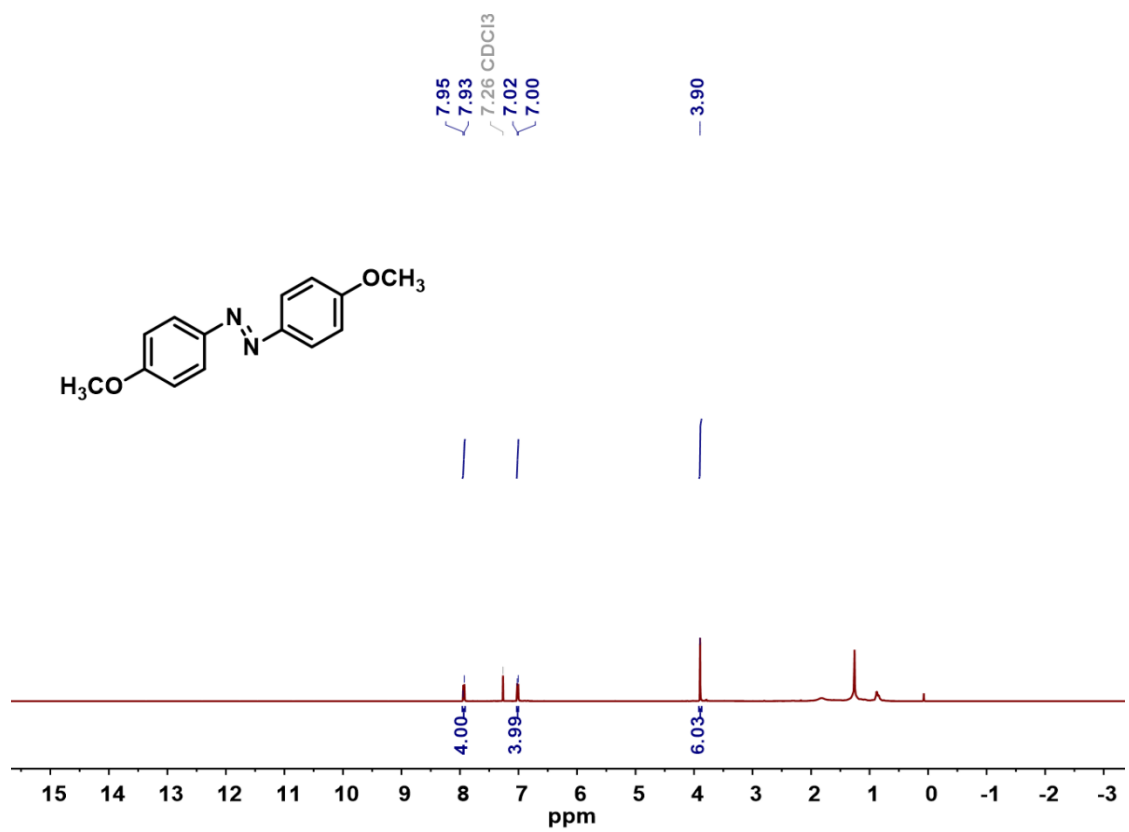


Fig. S20 ¹H and ¹³C NMR spectra of 1,2-bis(4-methoxyphenyl)diazene.

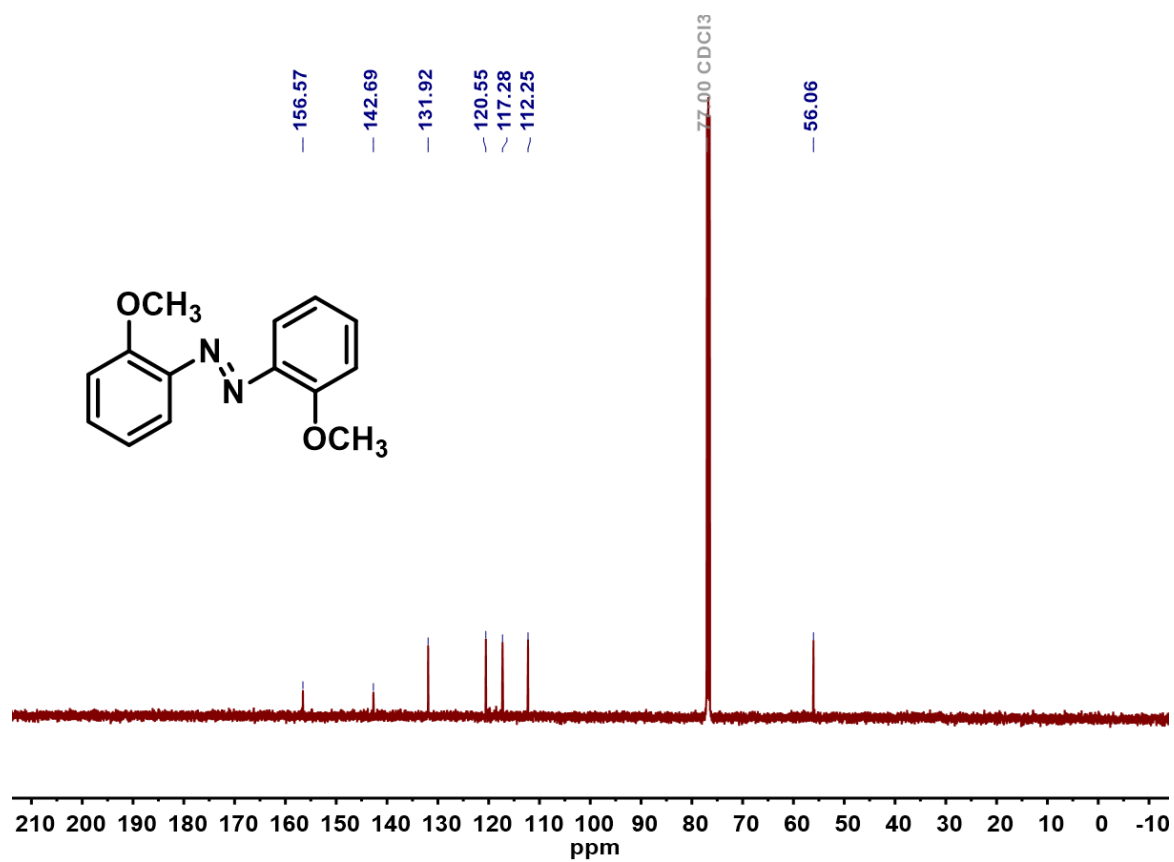
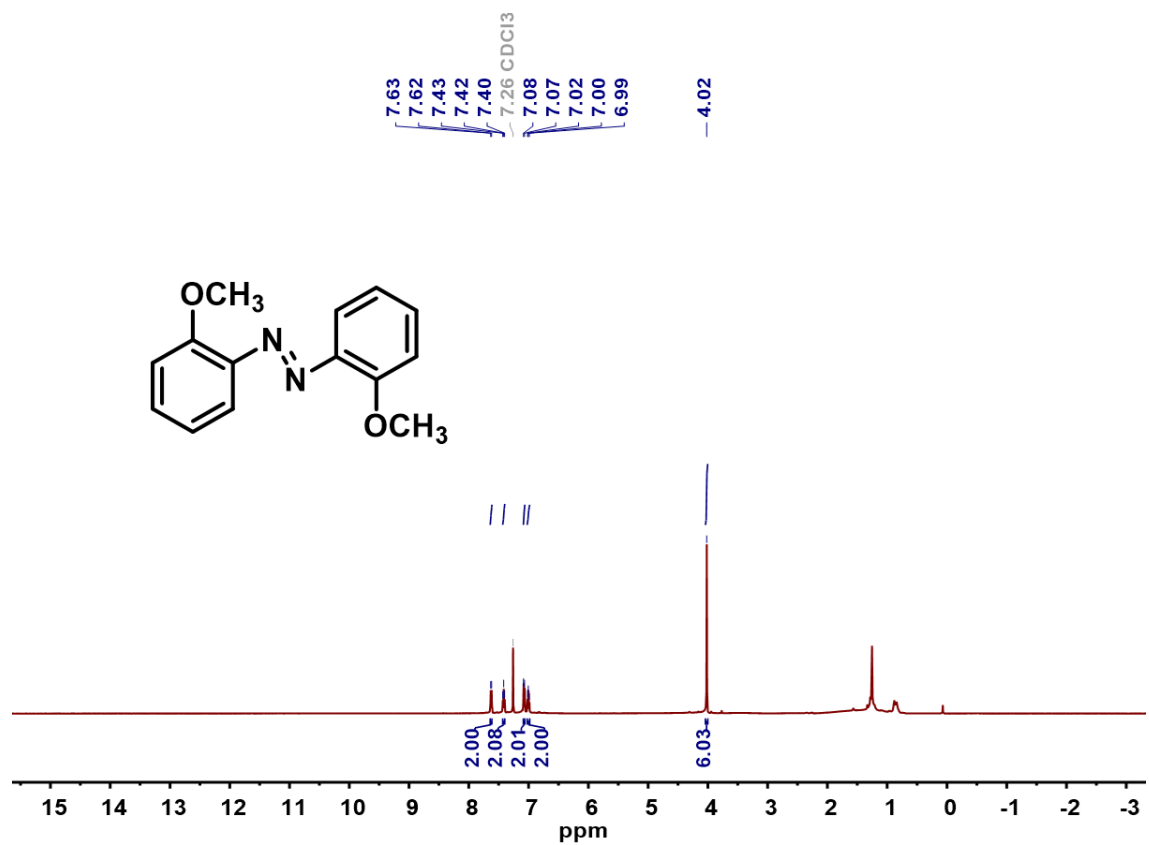


Fig. S21 ¹H and ¹³C NMR spectra of 1,2-bis(2-methoxyphenyl)diazene.

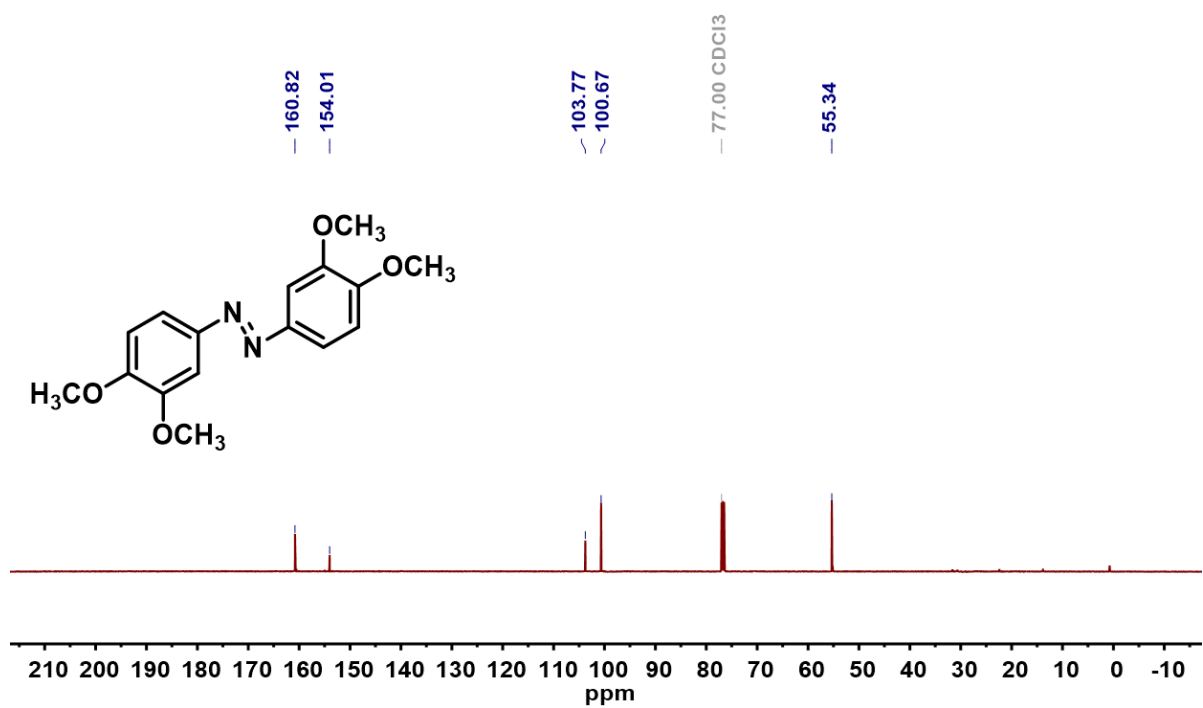
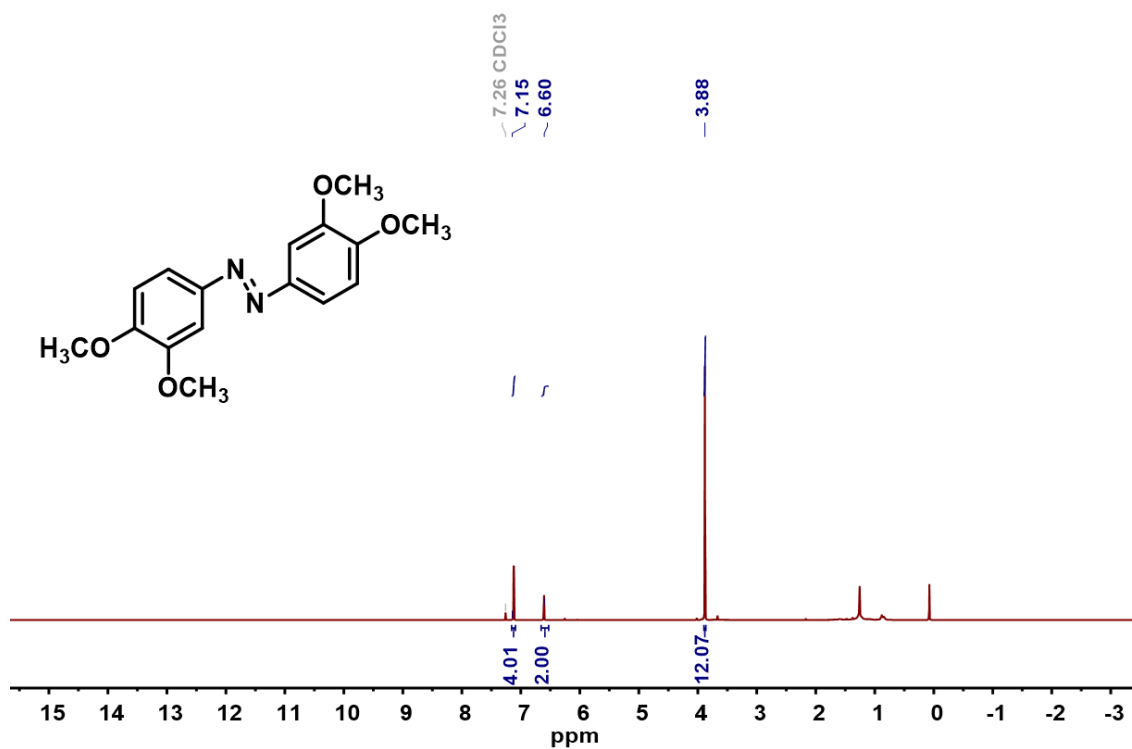


Fig. S22 ¹H and ¹³C NMR spectra of 1,2-bis(3,5-dimethoxyphenyl)diazene.

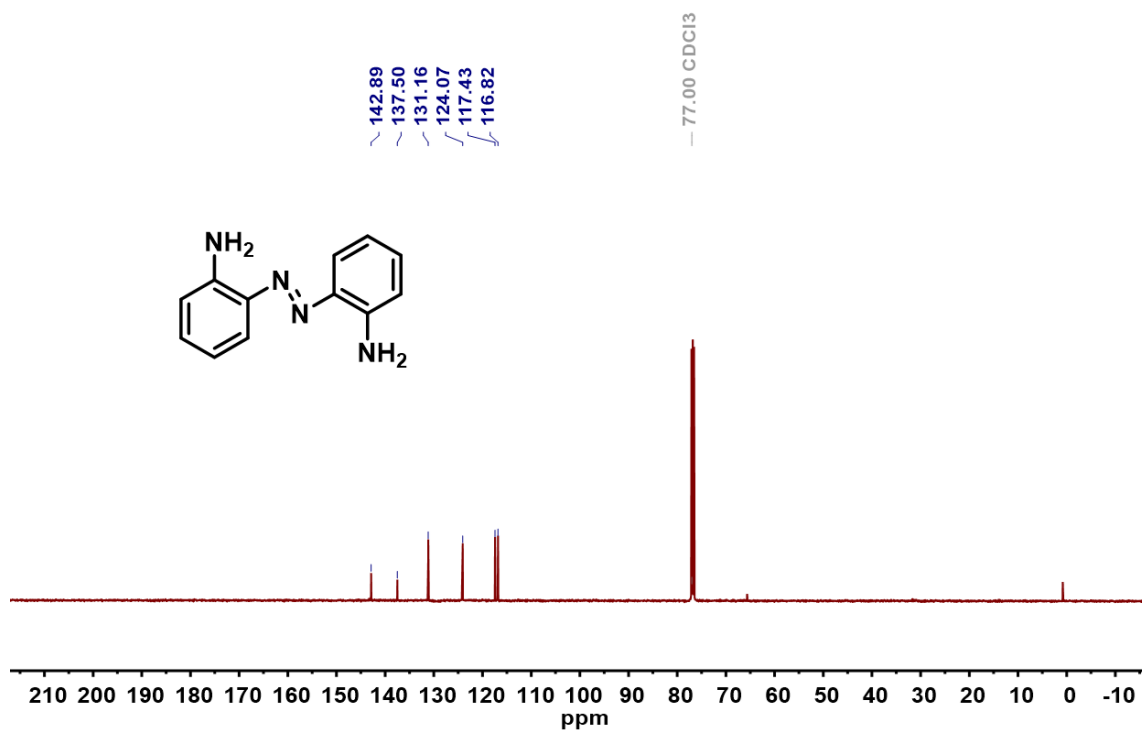
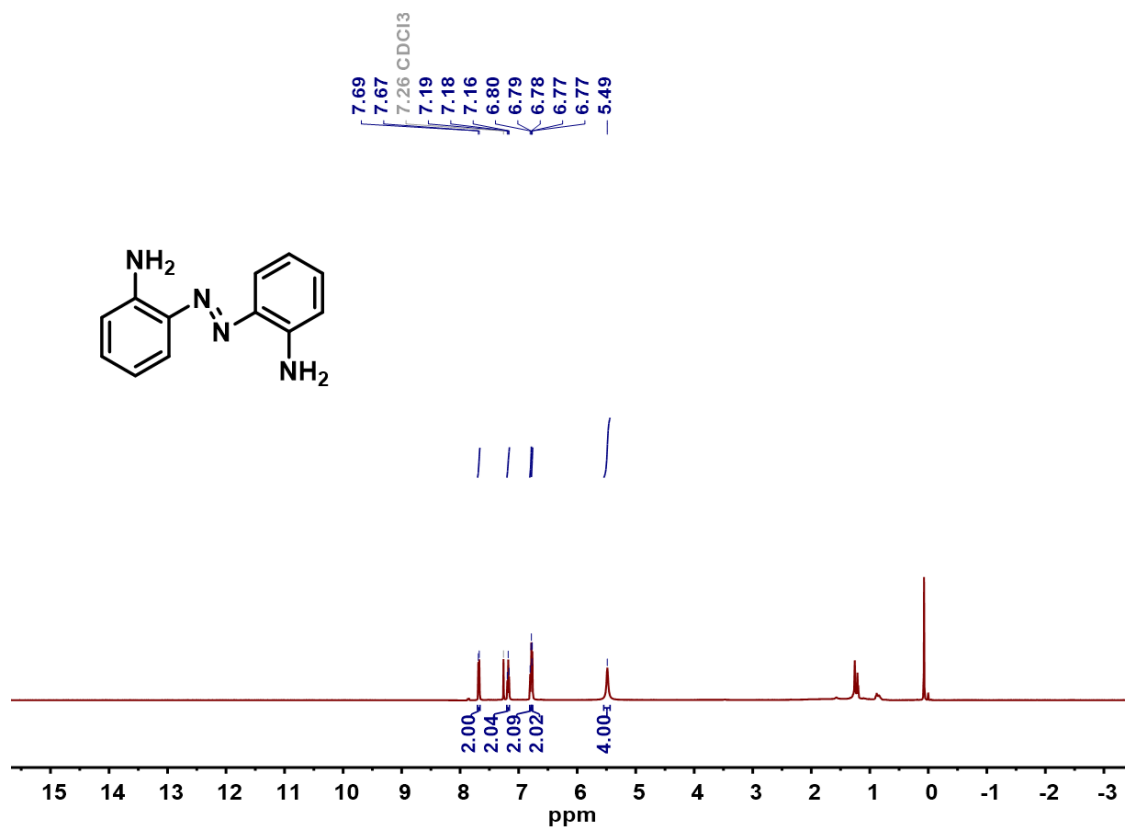


Fig. S23 ¹H and ¹³C NMR spectra of 1,2-bis(2-aminophenyl)diazene.

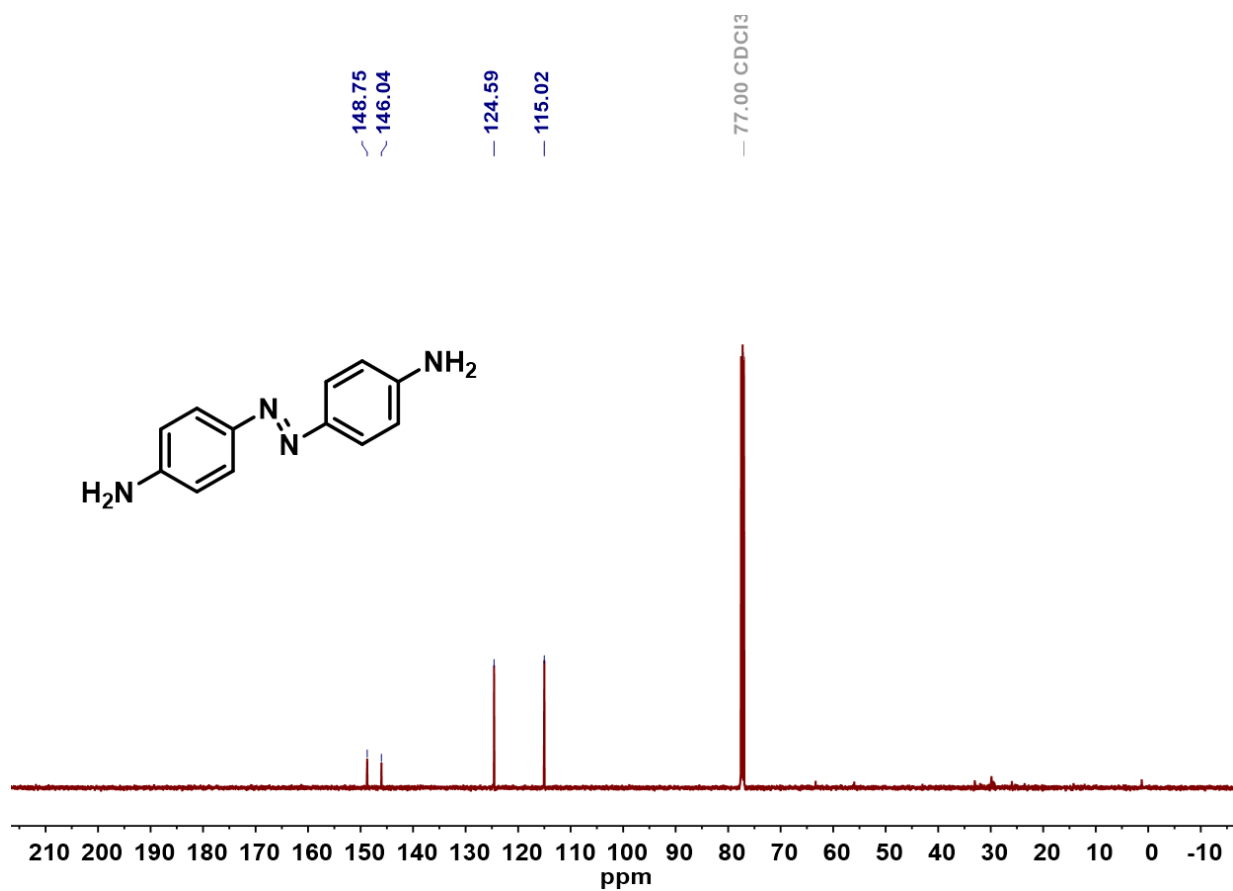
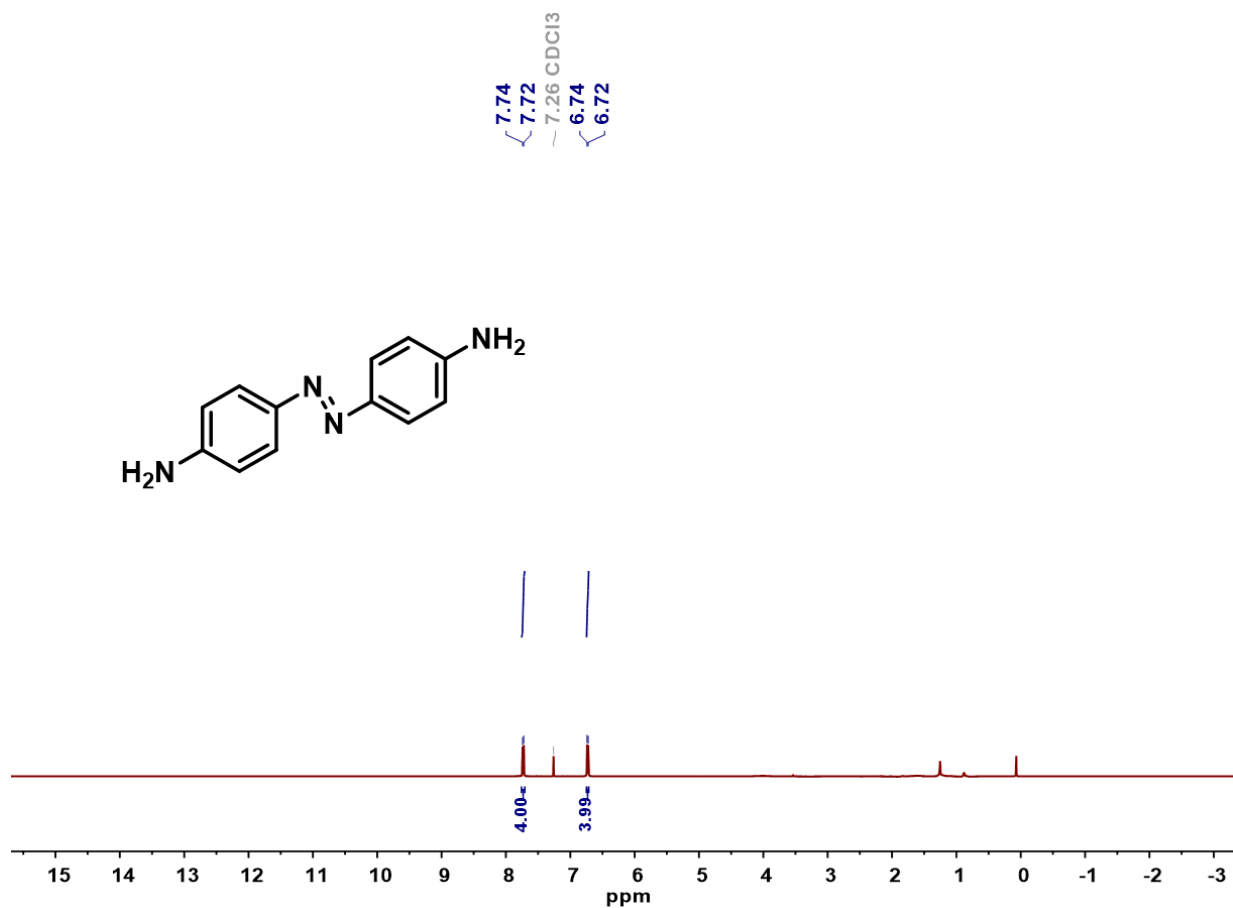


Fig. S24 ¹H and ¹³C NMR spectra of 1,2-bis(4-aminophenyl)diazene.

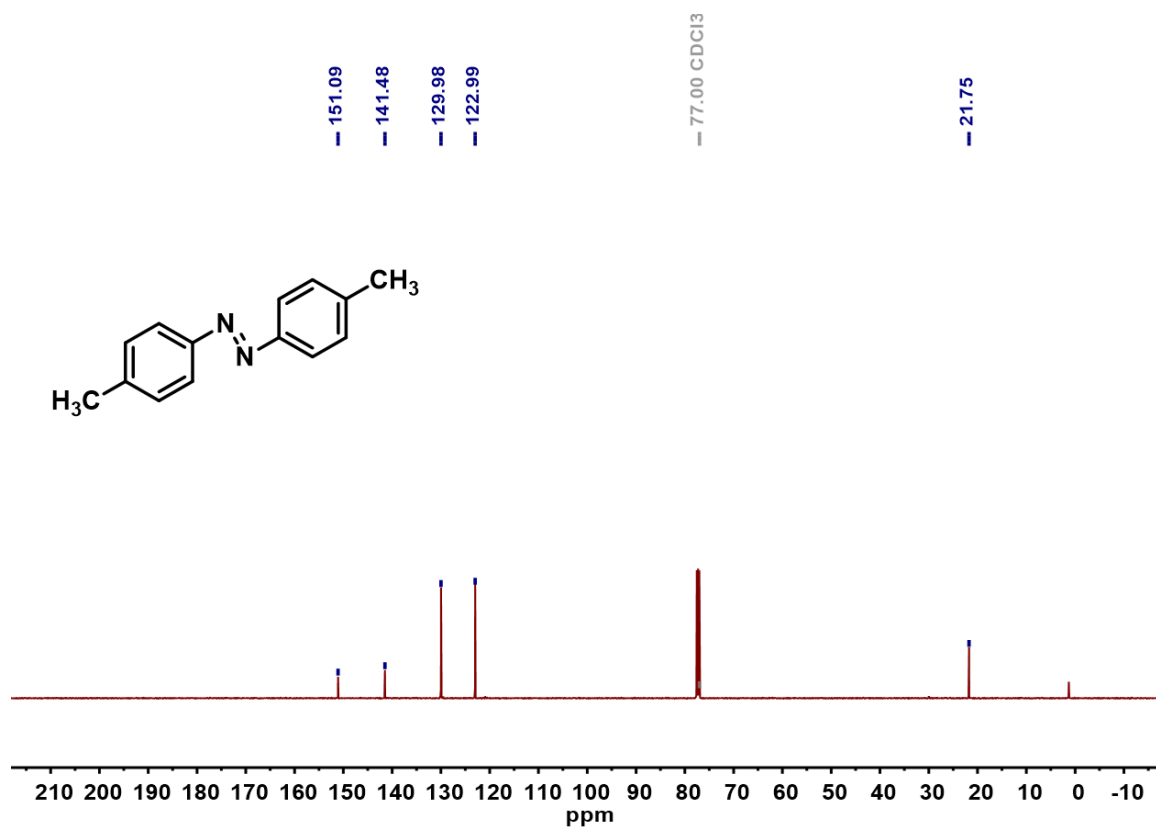
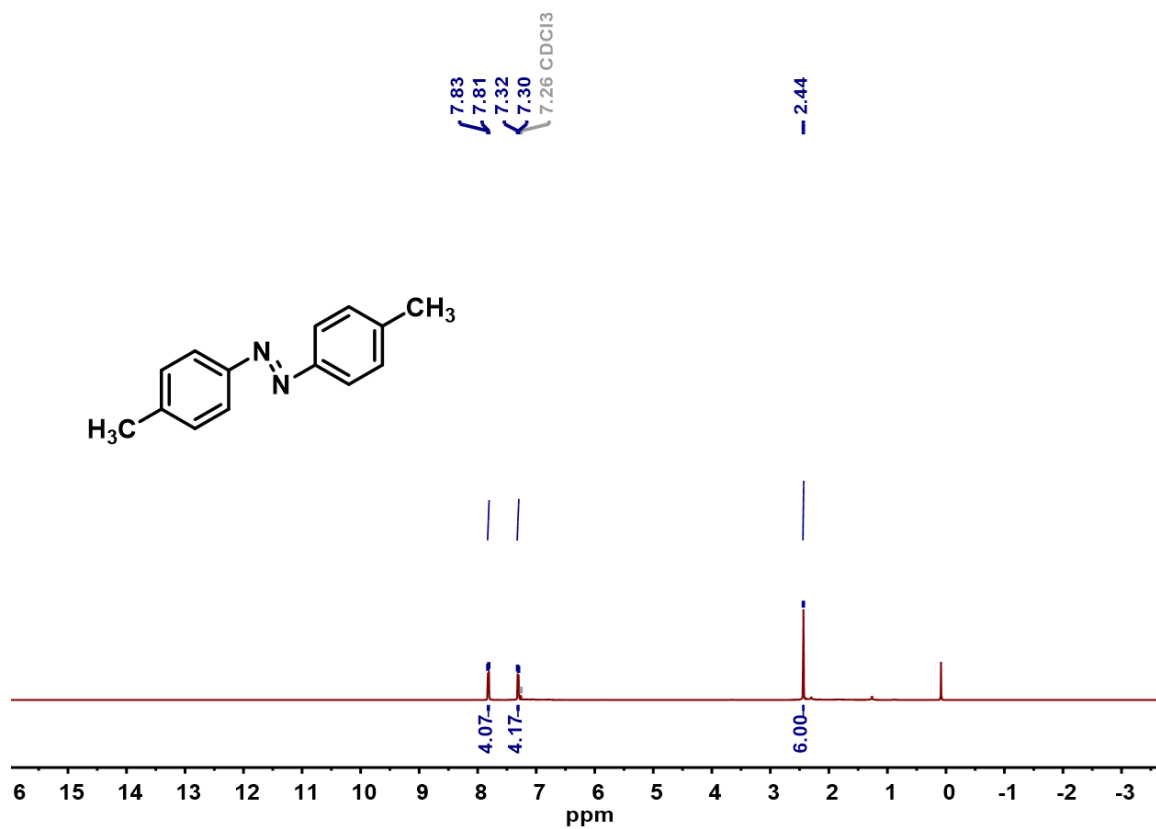


Fig. S25 ¹H and ¹³C NMR spectra of 1,2-bis(4-methylphenyl)diazene.

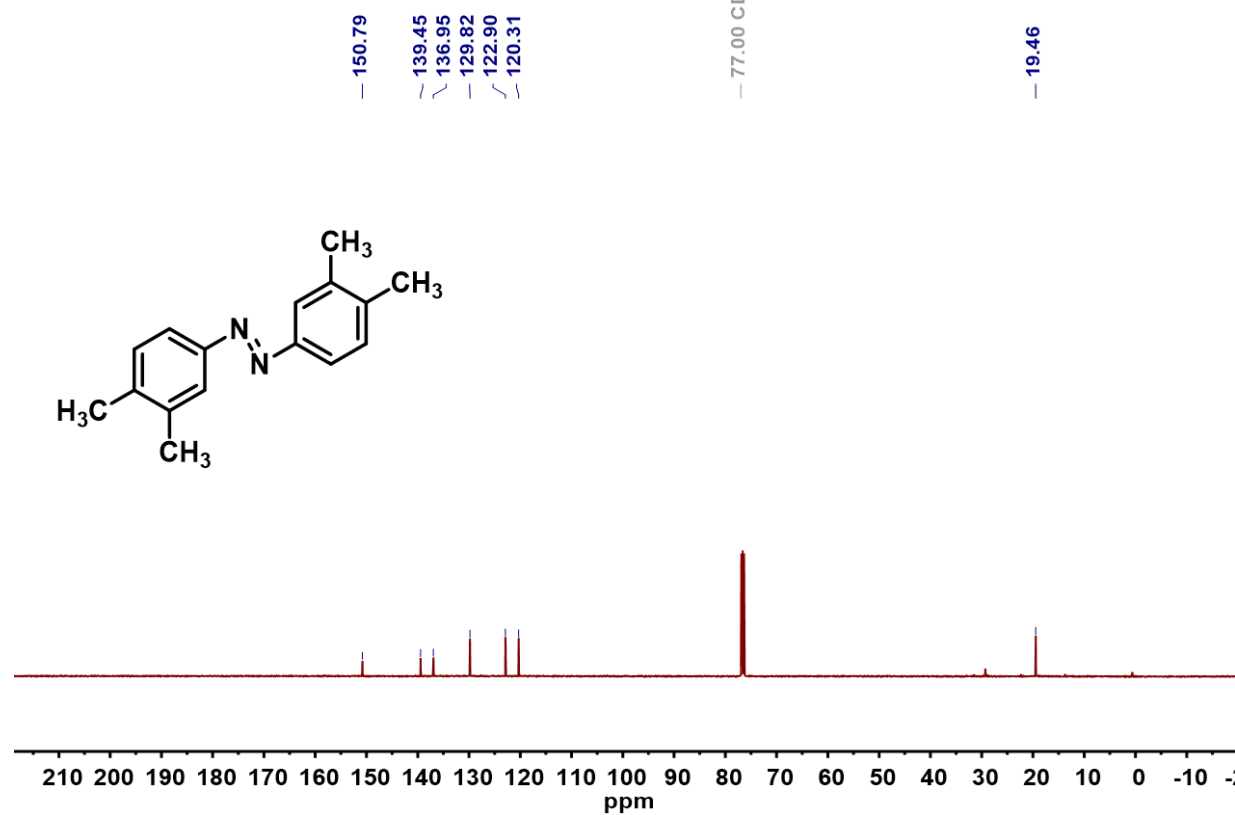
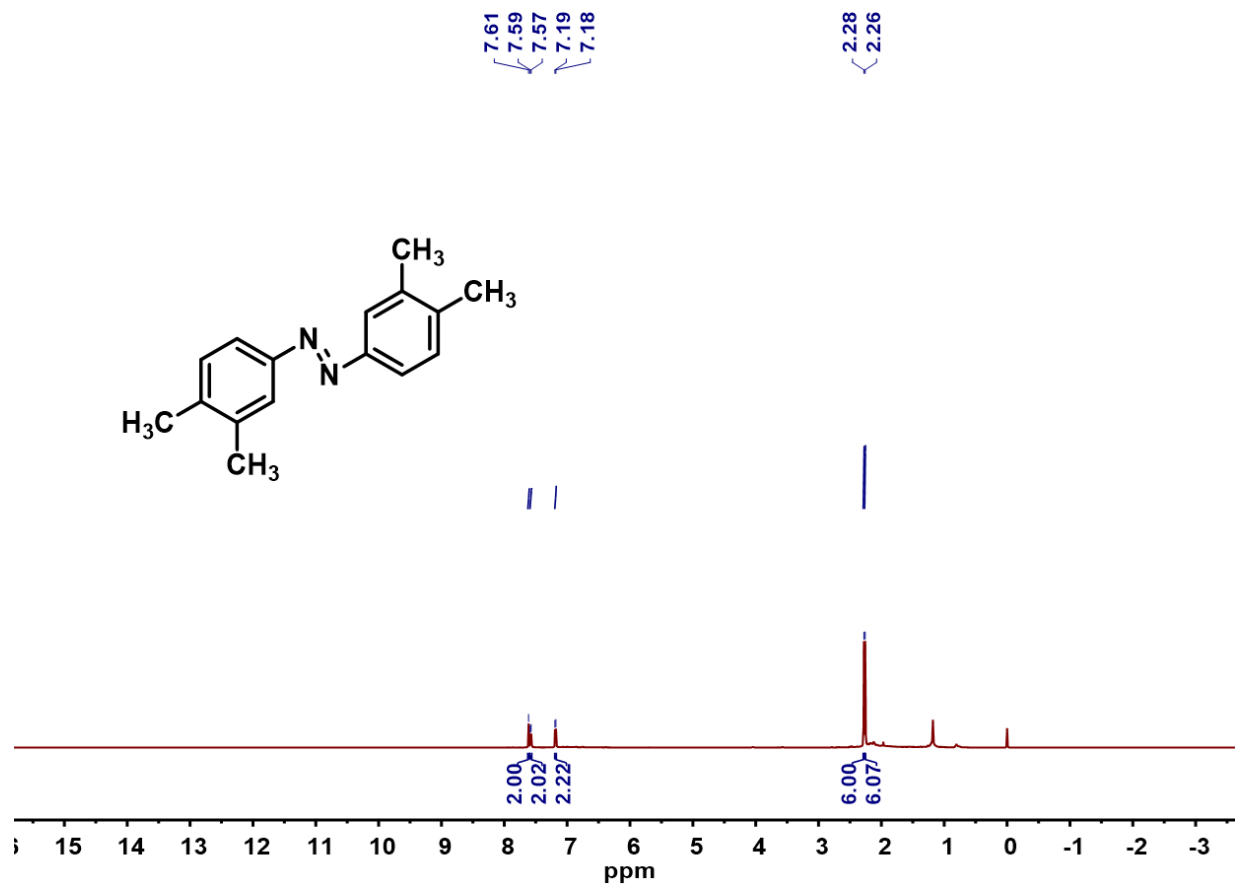


Fig. S26 ¹H and ¹³C NMR spectra of 1,2-bis(3,4-dimethylphenyl)diazene.

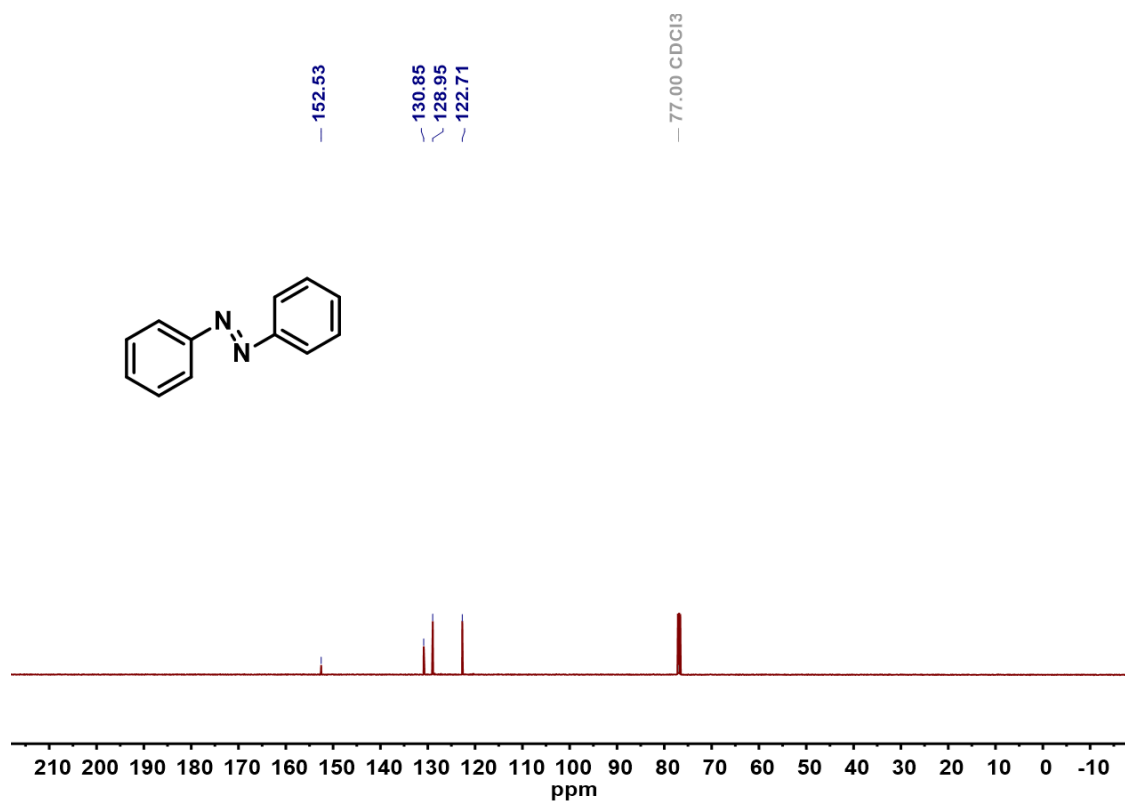
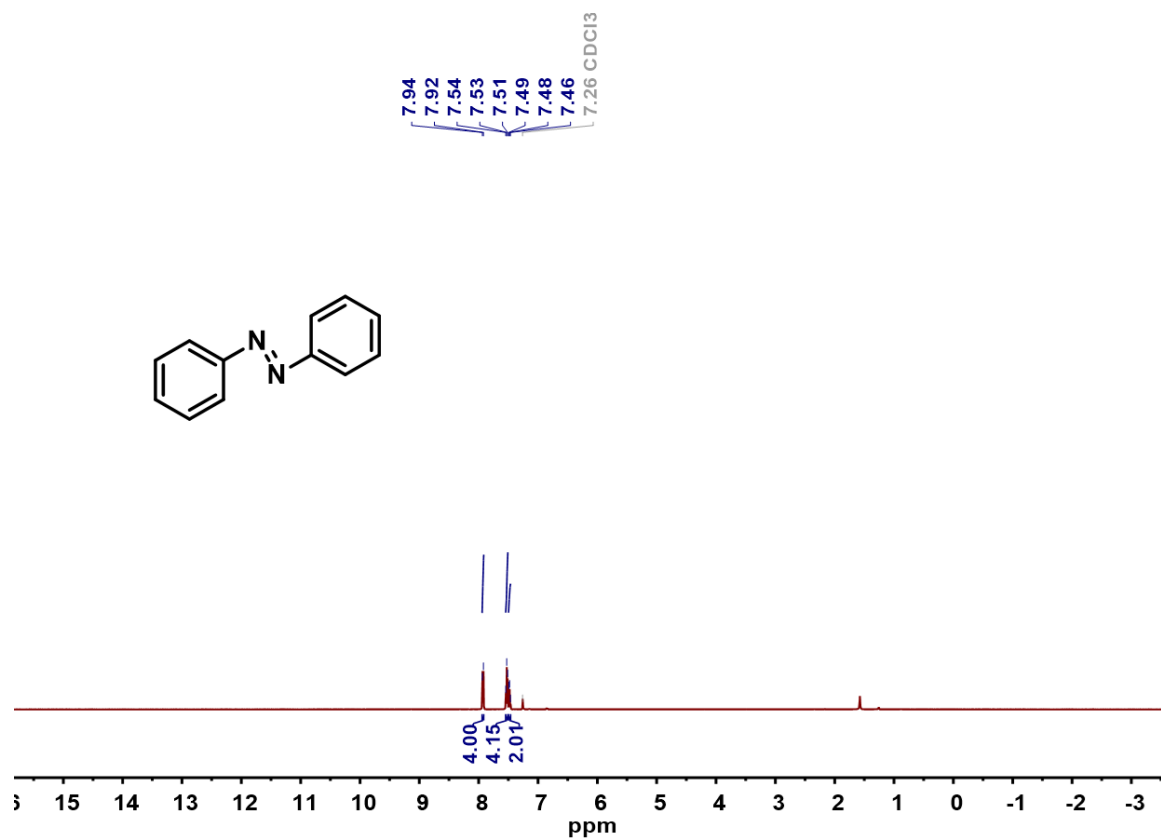


Fig. S27 ¹H and ¹³C NMR spectra of 1,2-diphenyldiazene.

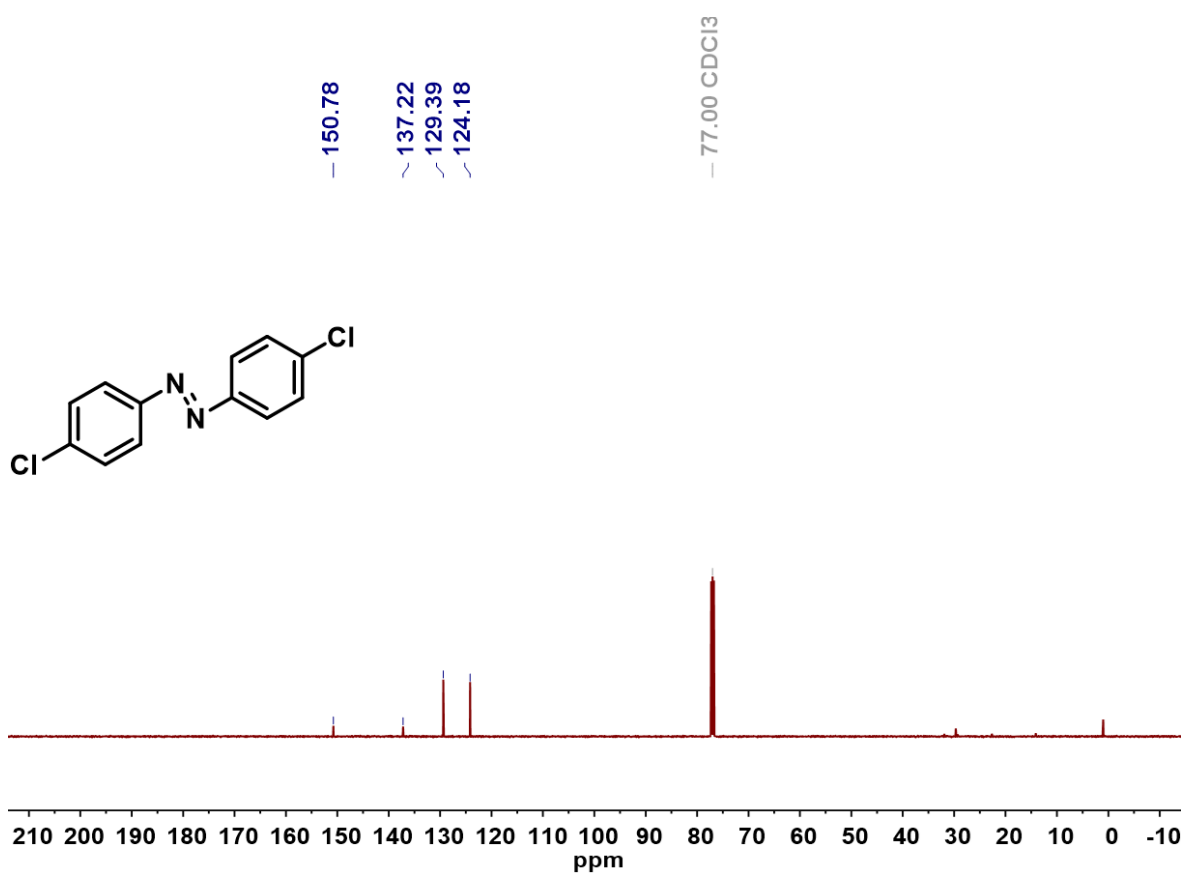
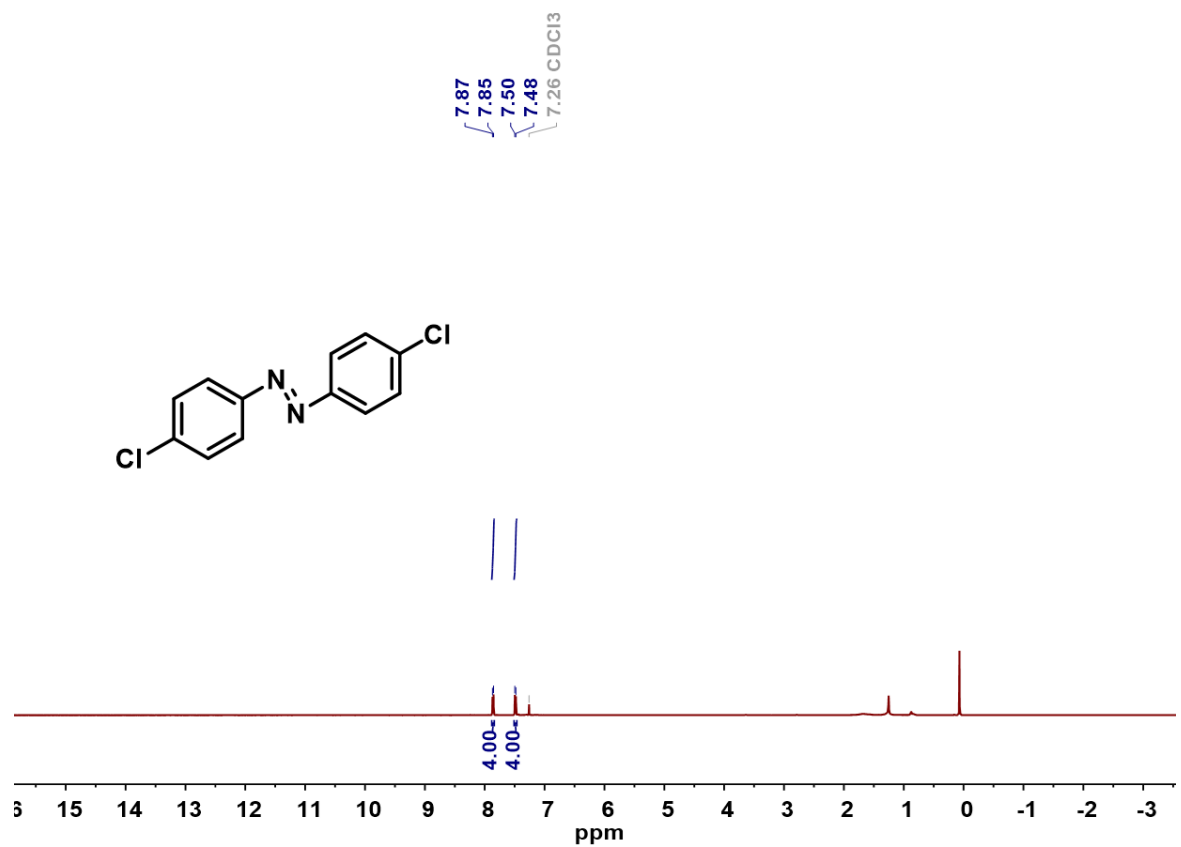


Fig. S28 ^1H and ^{13}C NMR spectra of 1,2-bis(4-chlorophenyl)diazene.

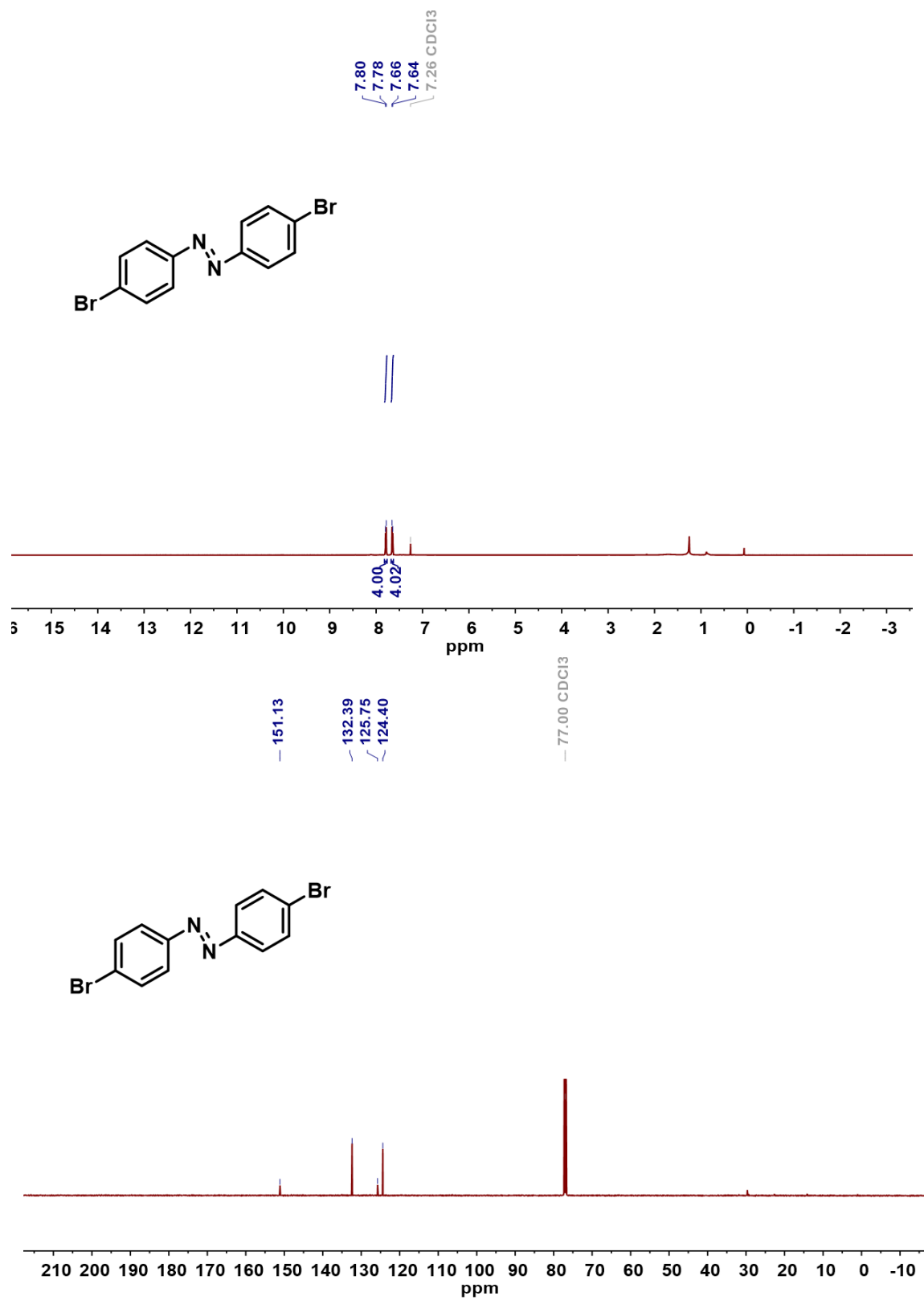


Fig. S29 ¹H and ¹³C NMR spectra of 1,2-bis(4-bromophenyl)diazene.

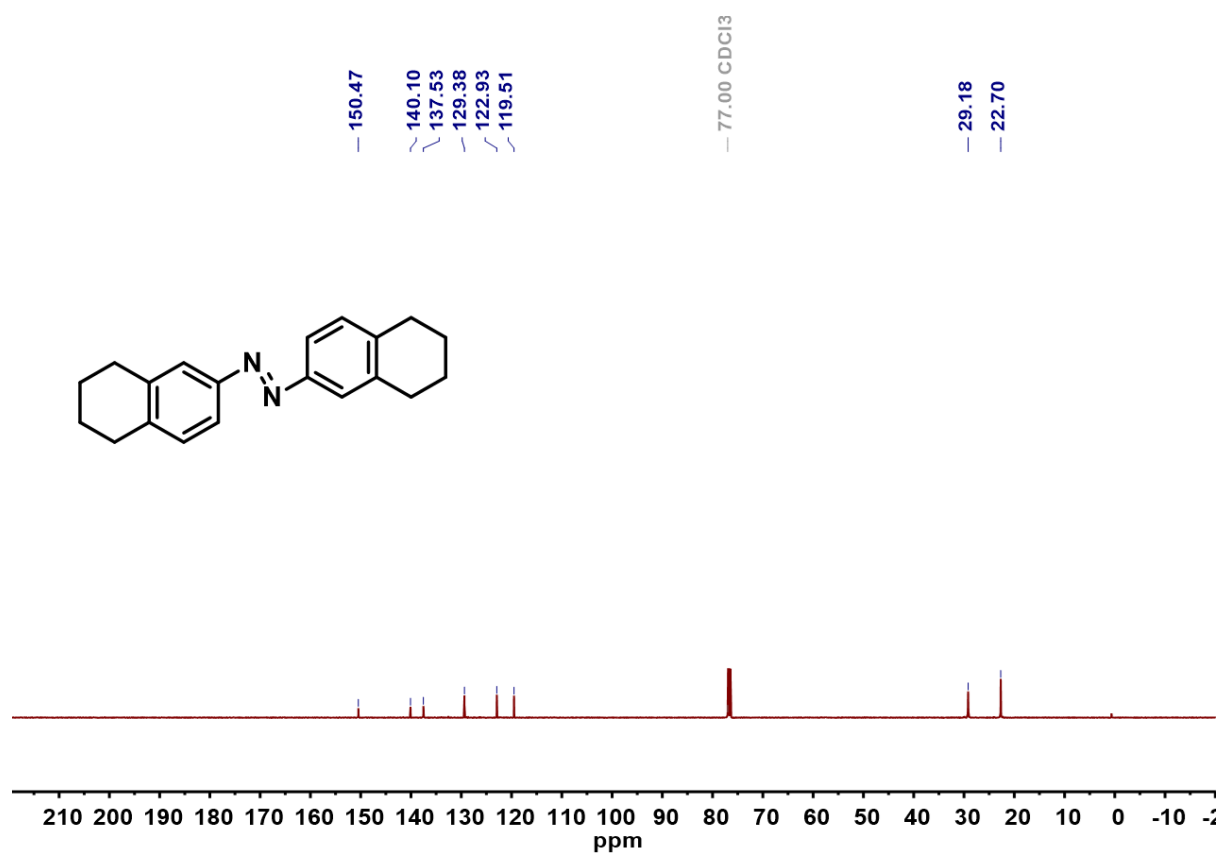
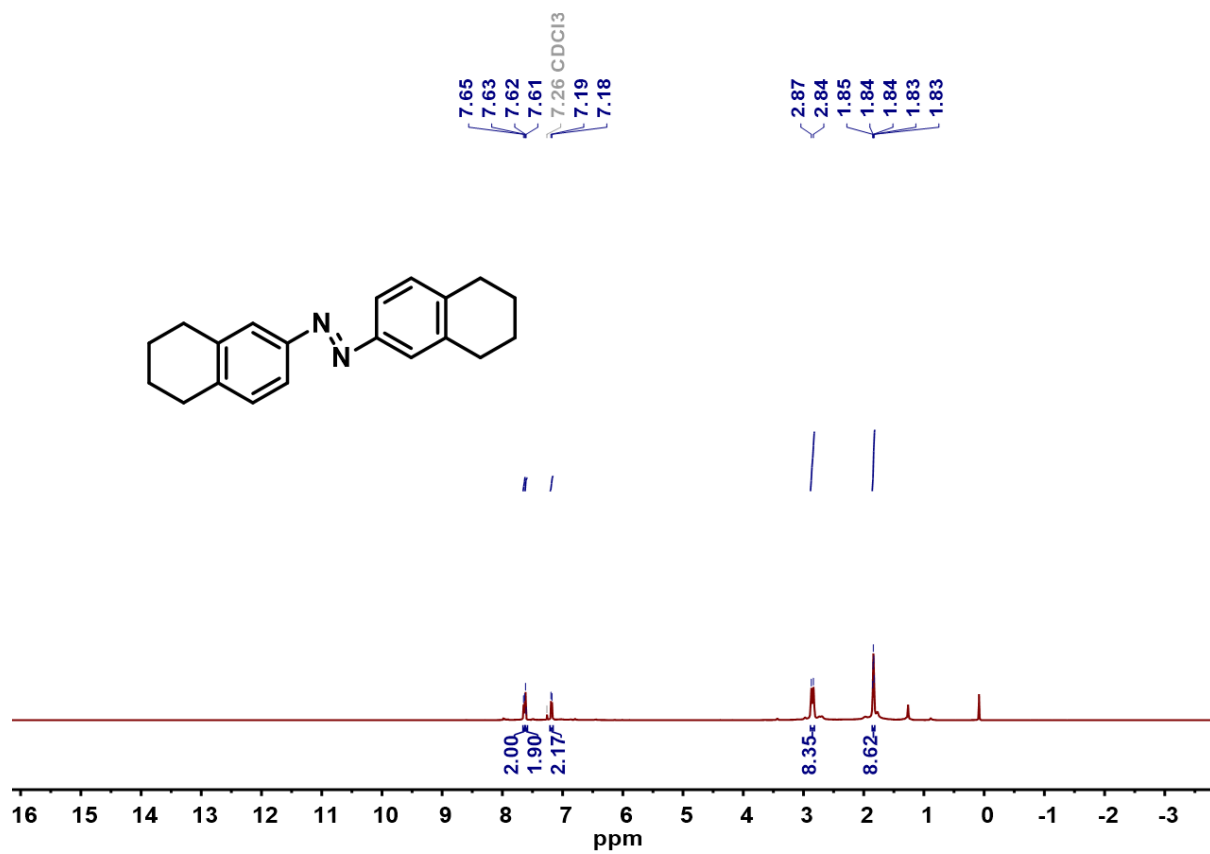


Fig. S30 ¹H and ¹³C NMR spectra of 1,2-bis(5,6,7,8-tetrahydronaphthalen-1-yl)diazene.

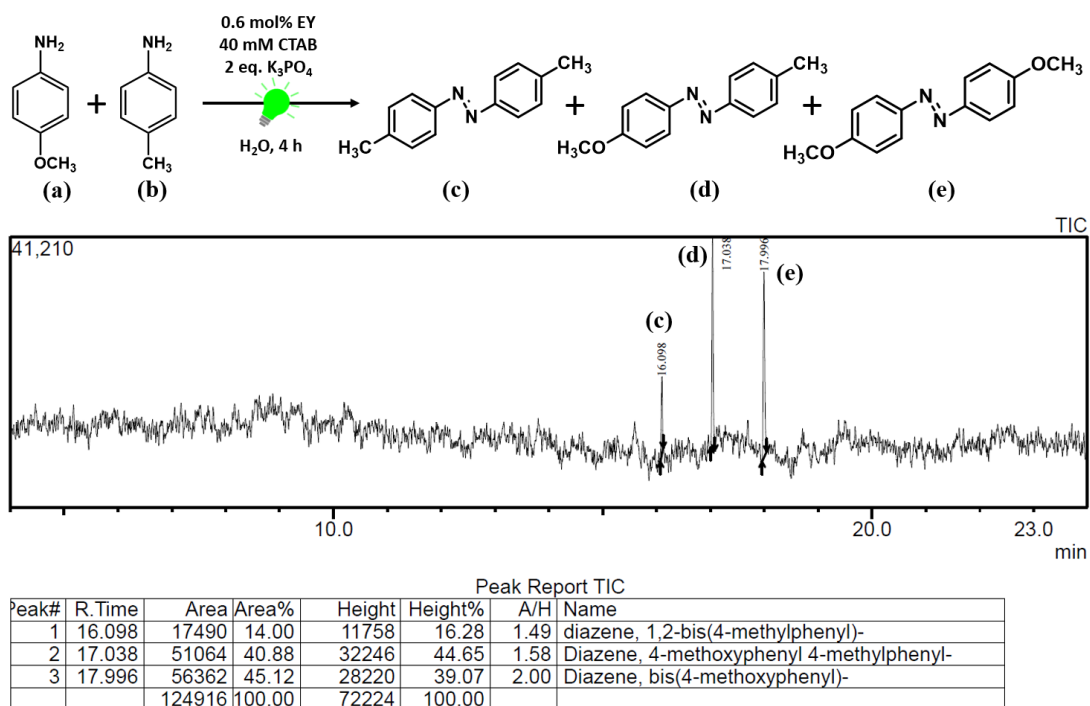


Fig. S31 GC-MS spectrum for the photocatalytic oxidative coupling of *p*-anisidine and *p*-toluidine.

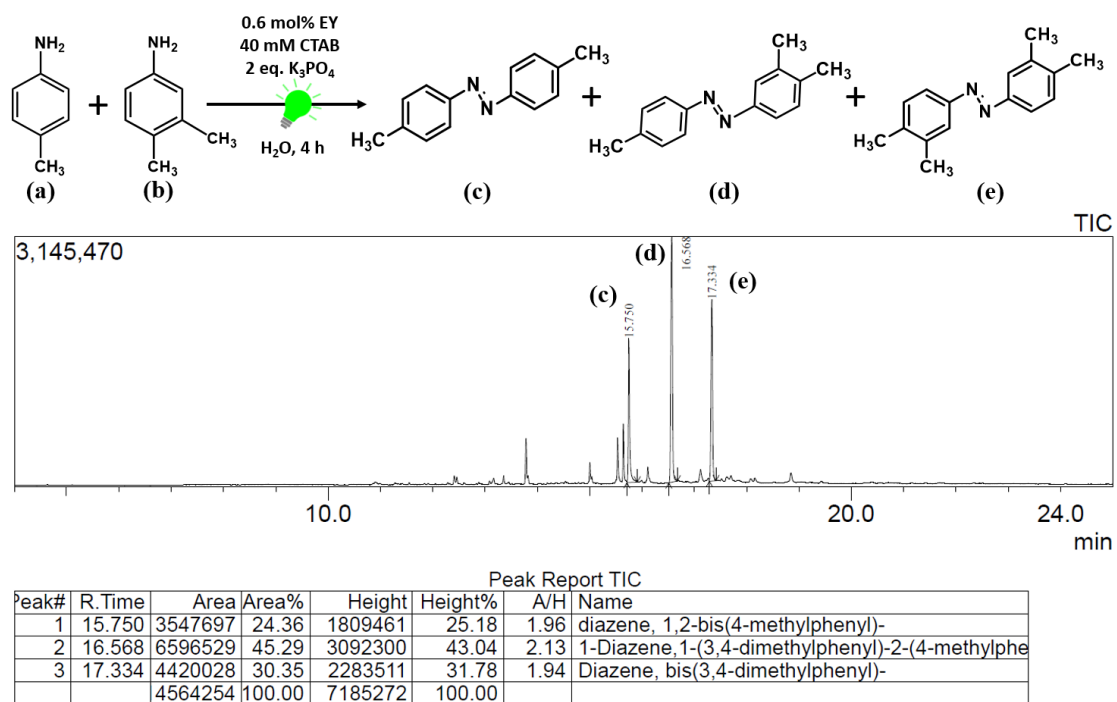


Fig. S32 GC-MS spectrum for the photocatalytic oxidative coupling of *p*-toluidine and 3,4-dimethylaniline.

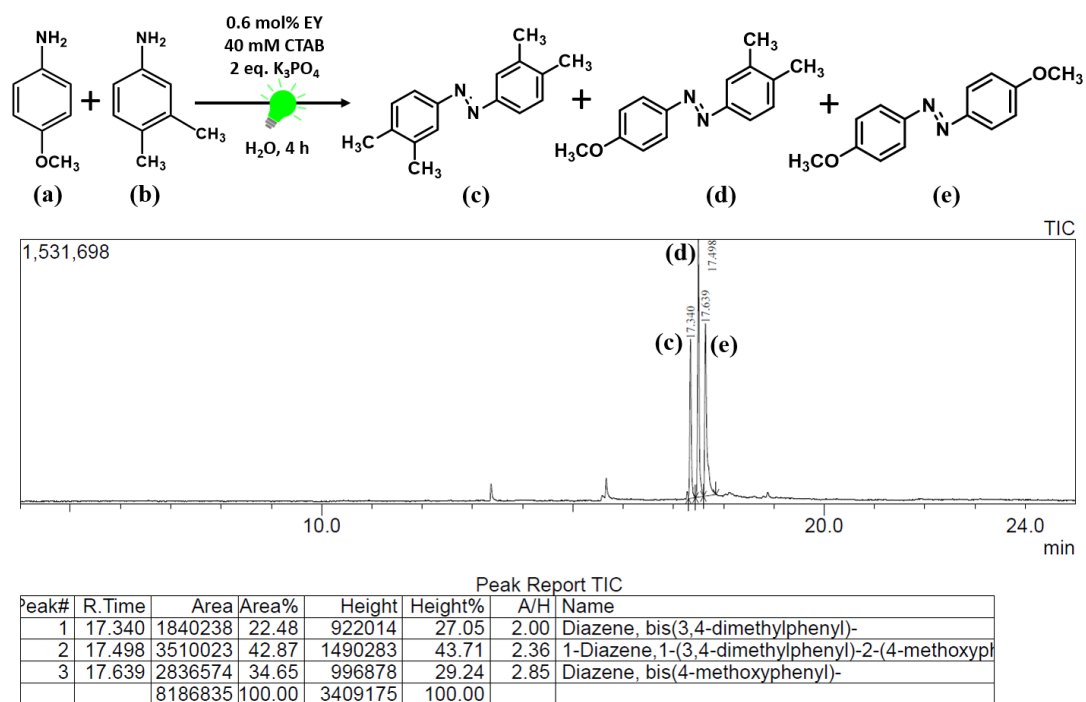


Fig. S33 GC-MS spectrum for the photocatalytic oxidative coupling of *p*-anisidine and 3,4-dimethylaniline.

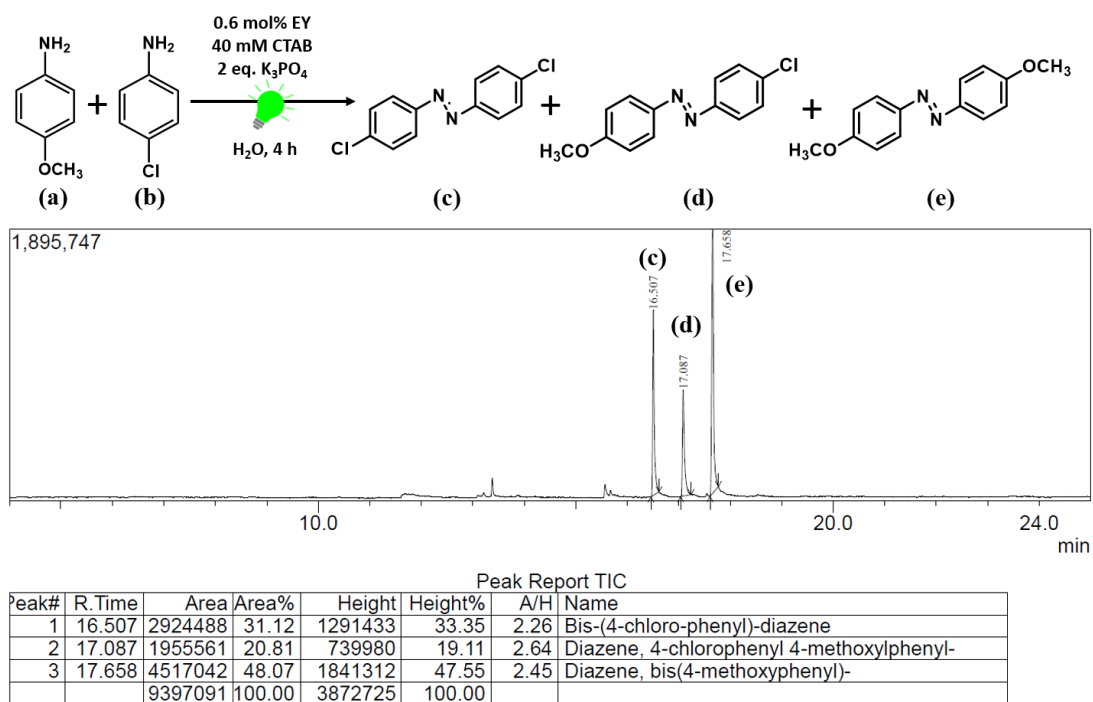


Fig. S34 GC-MS spectrum for the photocatalytic oxidative coupling of *p*-anisidine and *p*-chloroaniline.

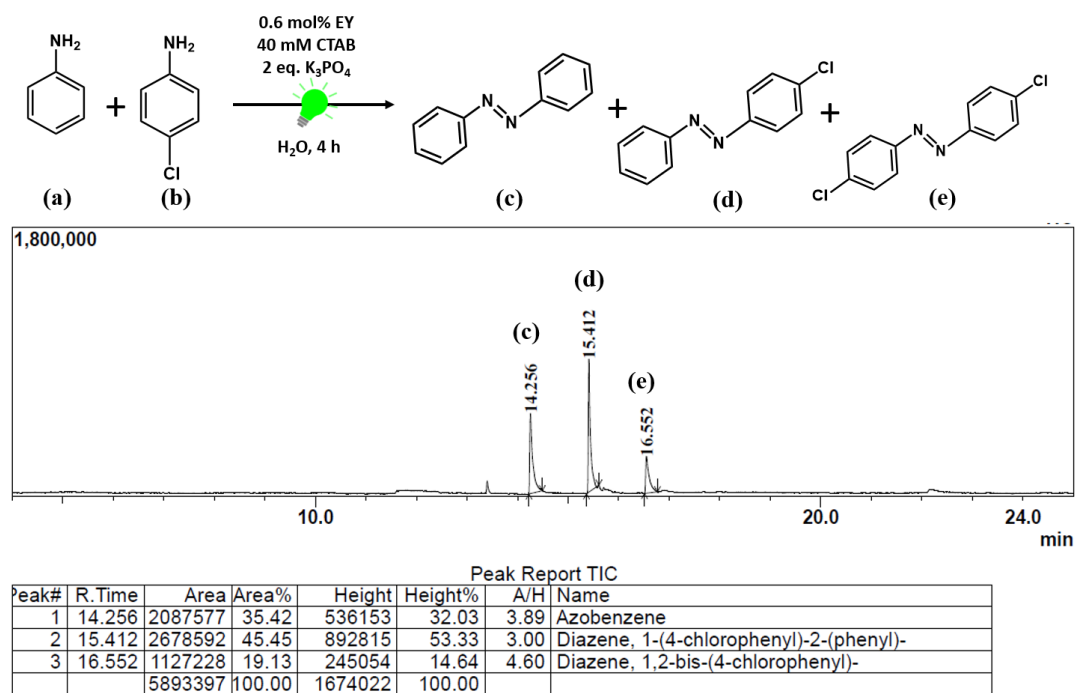
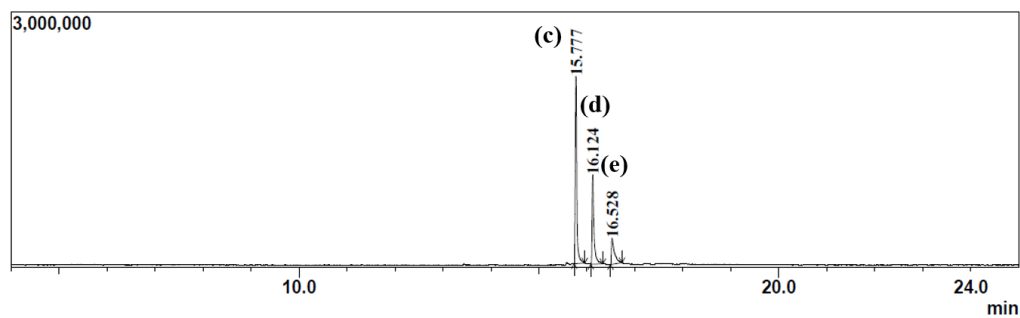
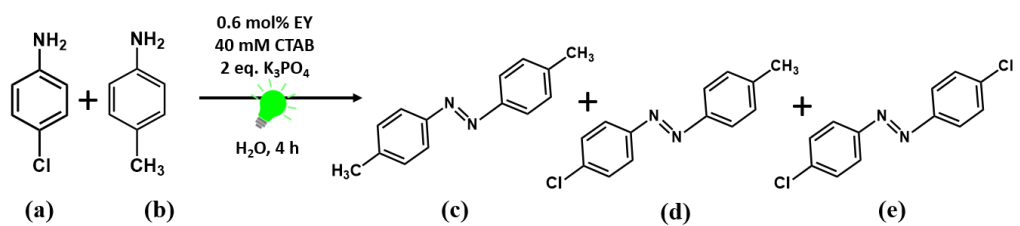


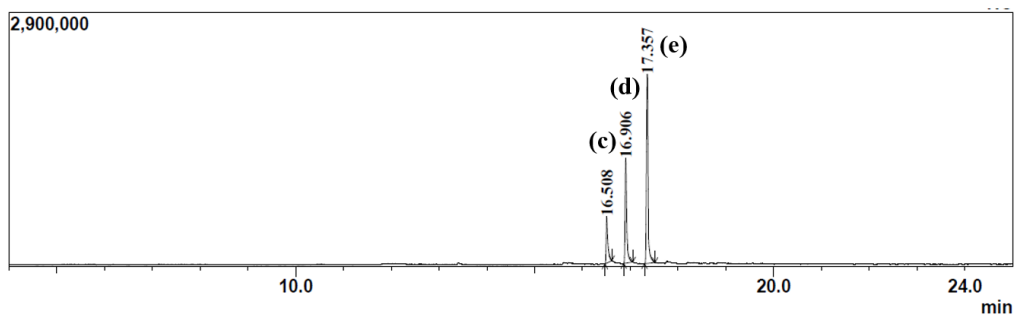
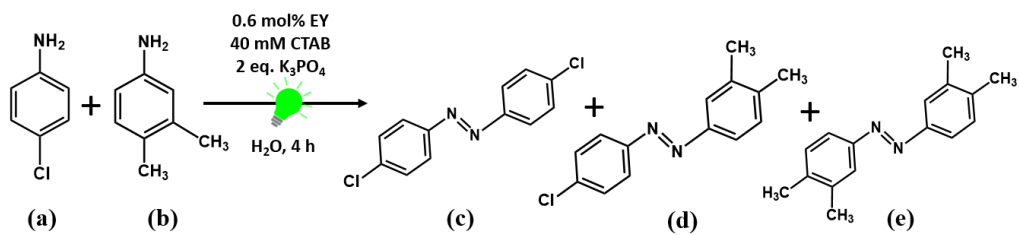
Fig. S35 GC-MS spectrum for the photocatalytic oxidative coupling of aniline and *p*-chloroaniline.



Peak Report TIC

Peak#	R.Time	Area	Area%	Height	Height%	A/H	Name
1	15.777	4781430	54.26	2205897	61.95	2.17	diazene, 1,2-bis(4-methylphenyl)-
2	16.124	2709092	30.74	1049759	29.48	2.58	diazene, 1-(4-chlorophenyl)-2-(4-methylphenyl)-
3	16.528	1322123	15.00	305375	8.58	4.33	diazene, 1,2-bis-(4-chlorophenyl)-
		8812645	100.00	3561031	100.00		

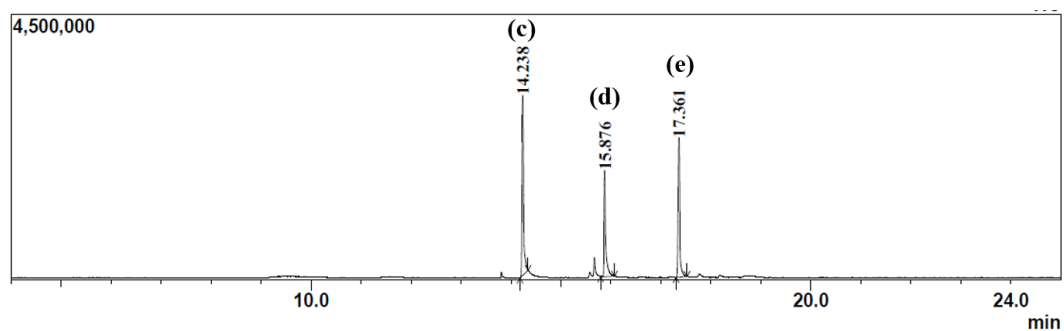
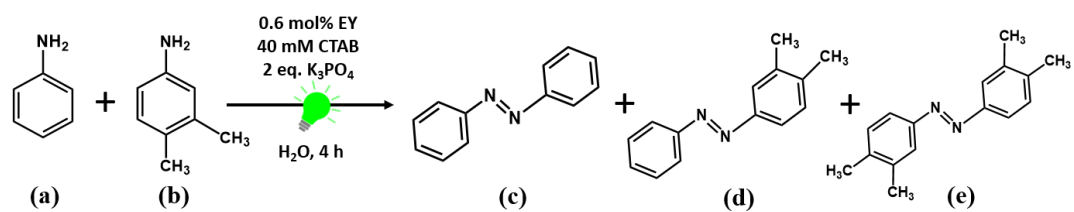
Fig. S36 GC-MS spectrum for the photocatalytic oxidative coupling of *p*-toluidine and *p*-chloroaniline.



Peak Report TIC

Peak#	R.Time	Area	Area%	Height	Height%	A/H	Name
1	16.508	1387892	14.92	532633	13.64	2.61	Diazene, 1,2-bis-(4-chlorophenyl)-
2	16.906	2721142	29.26	1204309	30.85	2.26	Diazene, 1-(4-chlorophenyl)-2-(3,4-dimethylphenyl)-
3	17.357	5191628	55.82	2166869	55.51	2.40	Diazene, bis(3,4-dimethylphenyl)-
		9300662	100.00	3903811	100.00		

Fig. S37 GC-MS spectrum for the photocatalytic oxidative coupling of *p*-chloroaniline and 3,4-dimethylaniline.



Peak Report TIC

Peak#	R.Time	Area	Area%	Height	Height%	A/H	Name
1	14.238	7231313	42.00	3063225	42.25	2.36	Azobenzene
2	15.876	4278326	24.85	1808754	24.95	2.37	Diazene, 1-(3,4-dimethylphenyl)-2-(phenyl)-
3	17.361	5706418	33.15	2378509	32.80	2.40	Diazene, bis(3,4-dimethylphenyl)-
		7216057	100.00	7250488	100.00		

Fig. S38 GC-MS spectrum for the photocatalytic oxidative coupling of aniline and 3,4-dimethylaniline.

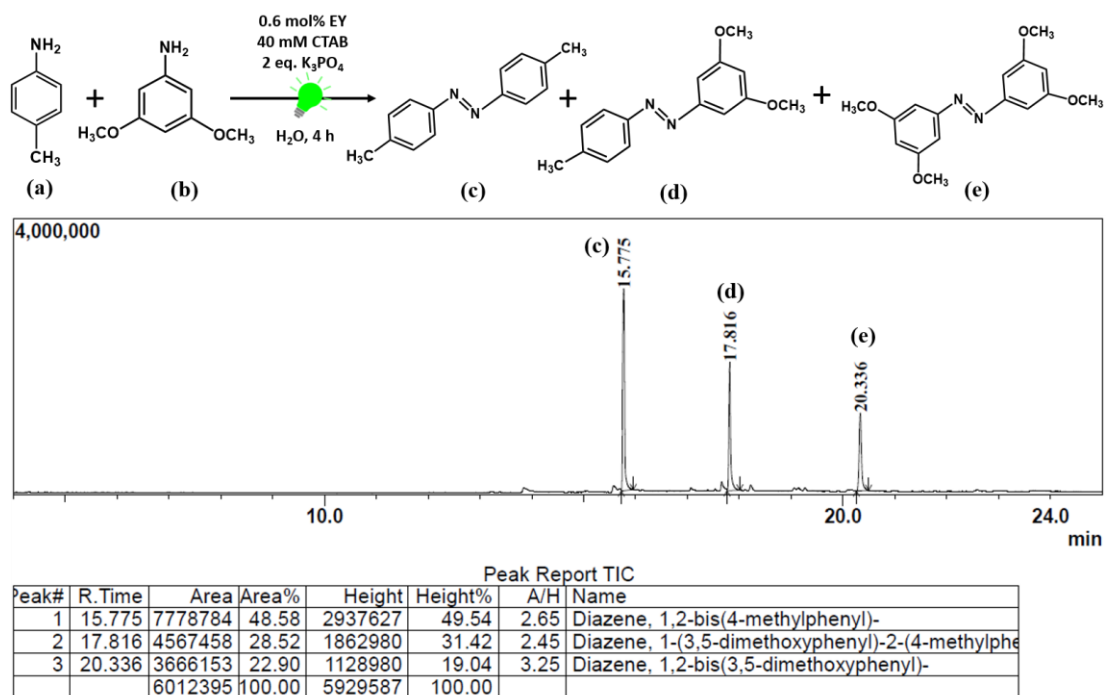


Fig. S39 GC-MS spectrum for the photocatalytic oxidative coupling of *p*-toluidine and 3,5-dimethoxyaniline .

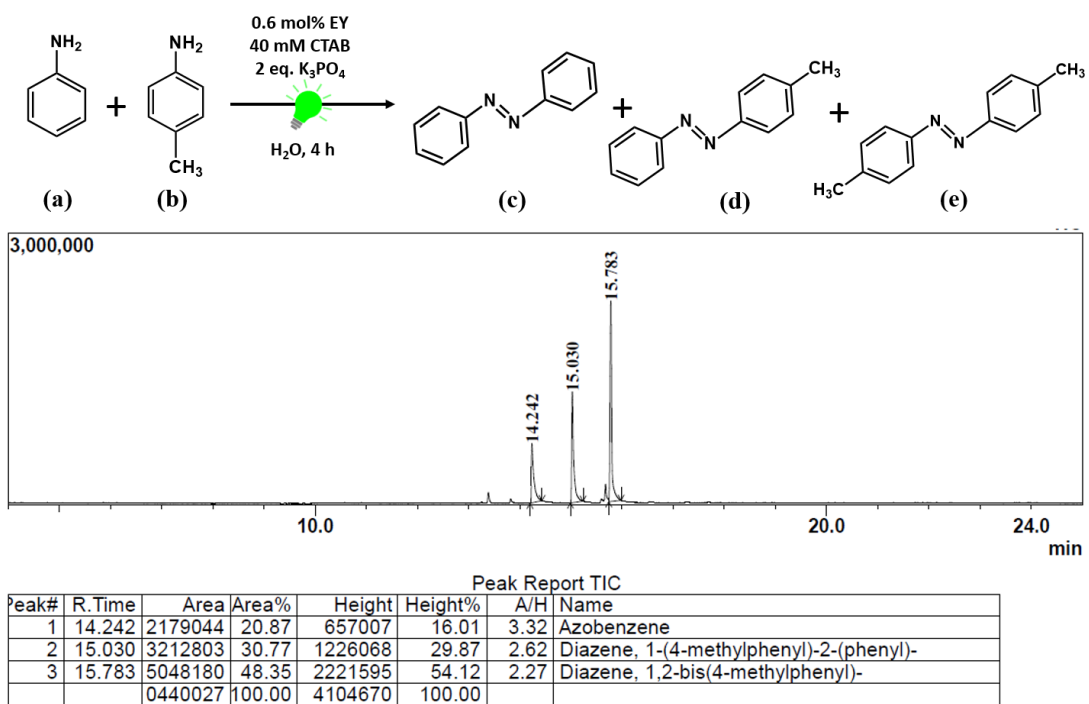


Fig. S40 GC-MS spectrum for the photocatalytic oxidative coupling of aniline and *p*-toluidine.

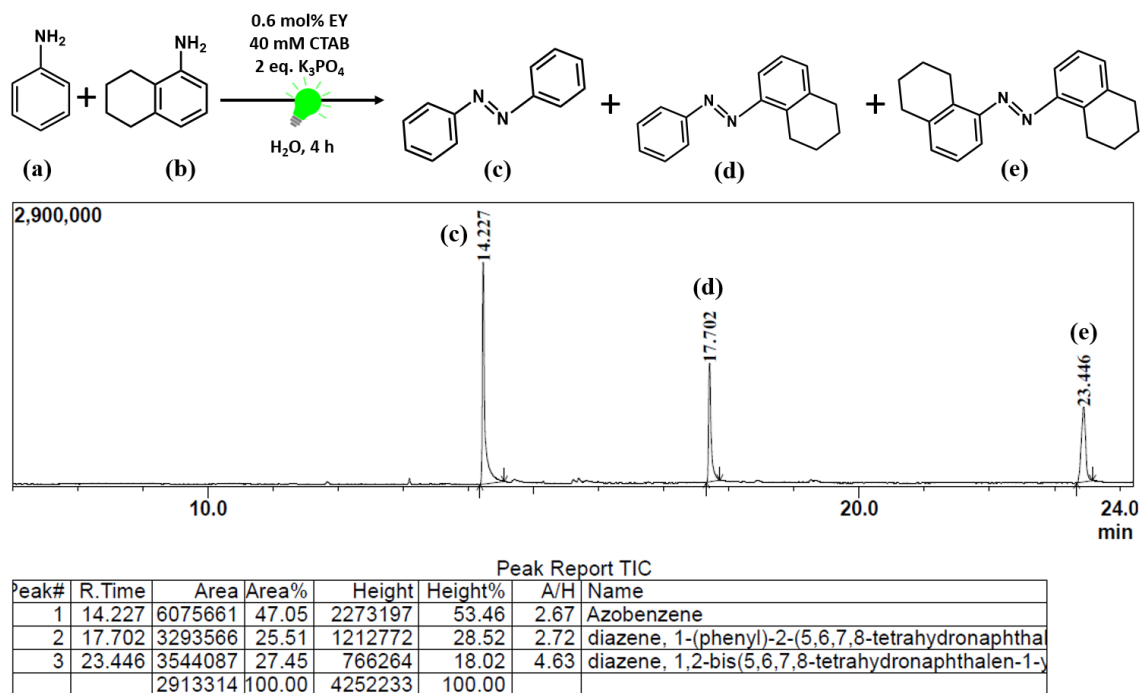


Fig. S41 GC-MS spectrum for the photocatalytic oxidative coupling of aniline and 5,6,7,8-tetrahydronaphthalen-1-amine.

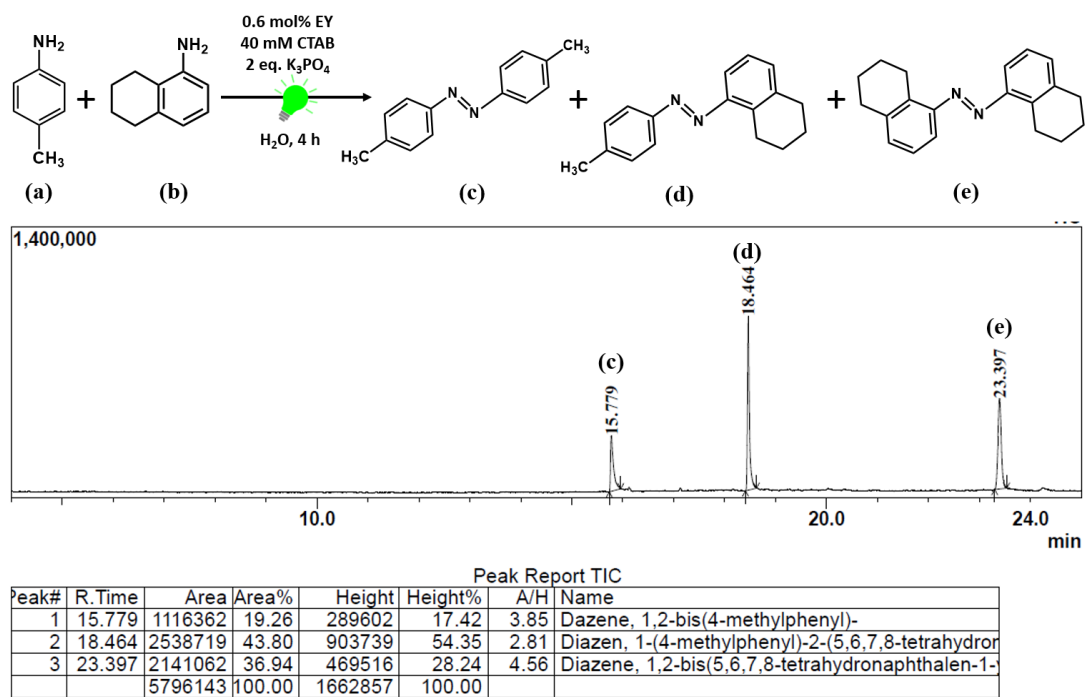


Fig. S42 GC-MS spectrum for the photocatalytic oxidative coupling of *p*-toluidine and 5,6,7,8-tetrahydronaphthalen-1-amine.

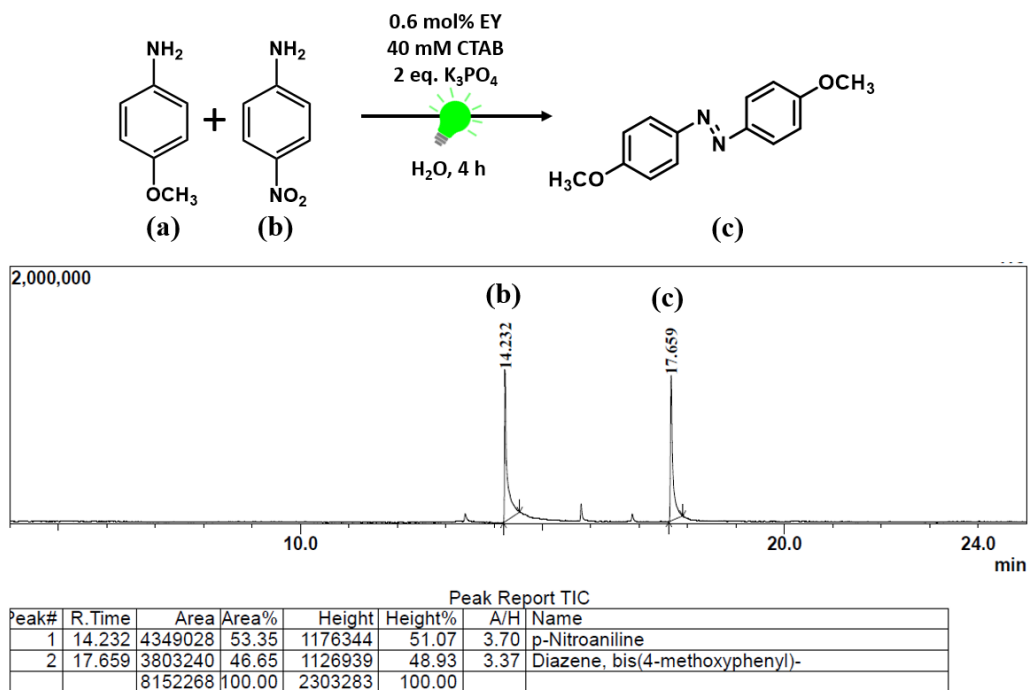


Fig. S43 GC-MS spectrum for the photocatalytic oxidative coupling of *p*-nitroaniline and *p*-anisidine.

Table S1 Micellization parameters of different surfactants.

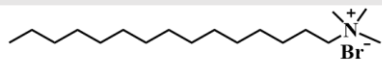
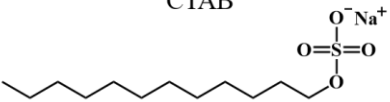
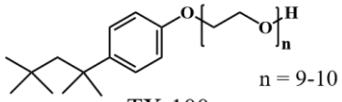
S.No.	Surfactant	CMC (mM)	Surface Charge
1.	 CTAB	0.9	positive
2.	 SDS	8	negative
3.	 TX-100 n = 9-10	0.24	non-ionic

Table S2 Fluorescence lifetime decay parameters of EY in the presence of CTAB and K₃PO₄ estimated from TCSPC measurements.

S. No.	Sample	τ_1 (ns)	a_1	$\langle\tau\rangle$ (ns)	χ^2
1.	EY	1.17	1	1.17	1.04
2.	CTAB + EY	2.74	1	2.74	1.14
3.	CTAB + EY + K ₃ PO ₄	2.76	1	2.76	1.16

Table S3 Fluorescence quenching parameters of EY@CTAB in the presence of different substrates.

S.No.	Substrates	K_{SV} (10^4 M^{-1})	k_q ($10^{12} \text{ M}^{-1} \text{ s}^{-1}$)
1.	<i>p</i> -anisidine	1.73	6.3
2.	aniline	1.62	5.9
3.	<i>p</i> -chloroaniline	1.34	4.9
4.	<i>p</i> -bromoaniline	0.90	3.3

Table S4 Fluorescence lifetime decay parameters of EY@CTAB in the presence of *p*-anisidine.

S. No.	Sample	τ_1 (ns)	a_1	τ_2 (ns)	a_2	$\langle\tau\rangle$ (ns)	χ^2
1.	CTAB + EY	2.74	1	-	-	2.74	1.14
2.	CTAB + EY + <i>p</i> -anisidine	0.77	0.39	2.73	0.61	1.96	1.18

References

- (1) S. Singh, J. K. Vaishnav and T. K. Mukherjee, *ACS Appl. Nano Mater.* 2020, **3**, 3604–3612.
- (2) S. Banerjee, B. G. Maddala, F. Ali and A. Datta, *Phys. Chem. Chem. Phys.* 2019, **21**, 9512–9519.
- (3) E. Speckmeier, T. G. Fischer and K. Zeitler, *J. Am. Chem. Soc.* 2018, **140**, 15353–15365.